Arthritis

Danesch et al., J Arthritis 2014, 3:3
http://dx.doi.org/10.4172/2167-7921.1000136

Research Article Open Access

NEM® Brand Eggshell Membrane Effective in the Treatment of Pain Associated with Knee and Hip Osteoarthritis: Results from a Six Center, Open Label German Clinical Study

Ulrich Danesch[1]*, Marion Seybold[1], Reiner Rittinghausen[1], Walter Treibel[2] and Norman Bitterlich[3]

[1]*Weber and Weber GmbH and Co. KG, Biological Medicinal Products, Herrschinger Str. 33, D-82266 Inning/Ammersee, Germany*
[2]*Orthopedic Practice, Maxhofstr. 9a, 81475 Munich, Germany*
[3]*Medizin and Service GmbH, Boettcherstr. 10, 09117 Chemnitz, Germany*

Abstract

Objective: NEM® brand eggshell membrane is a novel dietary supplement ingredient that contains naturally occurring glycosaminoglycans and proteins essential for maintaining healthy joints. A six center, open label clinical study was conducted to evaluate the efficacy and safety of NEM® as a treatment for pain and inflexibility associated with osteoarthritis of the knee and/or hip in a European population.

Methods: Forty-four subjects received oral NEM® 500 mg once daily for eight weeks. The primary outcome measure was to evaluate the mean effectiveness of NEM® in relieving general pain associated with moderate osteoarthritis of the knee and/or hip at 10,30 and 60 days utilizing a 10-question abbreviated questionnaire based on the WOMAC osteoarthritis questionnaire.

Results: Supplementation with NEM® produced a significant treatment response from baseline at 10 days (Q1-6 and Q9) (8.6% to 18.1% improvement) and at 30 and 60 days for all nine pain-related questions evaluated (22.4% to 35.6% improvement) and at 30 and 60 days for stiffness (Q10)(27.4% to 29.3% improvement). In a Patient's Global Assessment, greater than 59% of patients rated the efficacy of NEM® as good or very good following 60 days of supplementation. Physicians also rated the treatment effective in subjects, with greater than 75% having moderate or significant improvement from baseline after 60 days. There were no serious adverse events reported during the study and the treatment was reported to be well tolerated.

Conclusions: Supplementation with NEM® significantly reduced pain, both rapidly (10 days) and continuously (60 days) demonstrating that it is a safe and effective therapeutic option for the treatment of pain associated with osteoarthritis of the knee and/or hip. Results from previous clinical studies on NEM® can likely be extended to the broader European population.

Keywords: Knee, Hip, Osteoarthritis, Eggshell membrane, NEM, Dietary supplement, Glycosaminoglycans

Introduction

Estimates of the prevalence of osteoarthritis (OA) in European populations vary widely, however a recent study [1] from a region in Spain places the prevalence of knee OA at 12.2% and that of hip OA at 7.4%. The pain associated with these maladies can be quite debilitating and few treatment options exist outside of easing symptoms. This usually involves the use of analgesics (i.e. acetaminophen, oxycodone, propoxyphene) or non-steroidal anti-inflammatory drugs (NSAIDs) (i.e. ibuprofen, diclofenac, celecoxib), alone or in combination. Most of these treatments have shown limited effectiveness in randomized controlled clinical trials (RCTs) [2-5] or are known to have significant and sometimes severe side effects. NEM® brand eggshell membrane has previously demonstrated good efficacy in relieving pain and stiffness associated with OA of the knee in an RCT [6] and has shown similar efficacy in limited trials for other affected joints [7].

Eggshell membrane is primarily composed of fibrous proteins such as Collagen Type I [8]. However, eggshell membranes have also been shown to contain other bioactive components, namely glycosaminoglycans (i.e. dermatan sulfate, chondroitin sulfate and hyaluronic acid and keratan sulfate) [9-11]. A number of these constituents have been shown previously to be beneficial in the treatment of OA [12,13]. Eggshell membrane itself has been shown both *in vitro* [14] and *in vivo* [15] to reduce various pro-inflammatory cytokines, including interleukin-1 beta (IL-1β) and tumor necrosis factor alpha (TNF-α), two primary mediators of inflammation. A U.S. company, ESM Technologies, LLC (Carthage, MO USA), has developed methods to efficiently and effectively separate eggshell membrane from eggshells on a commercial metric-ton scale. The isolated membrane is then partially hydrolyzed using a proprietary process and dry-blended to produce NEM® brand eggshell membrane. Compositional analysis of NEM® conducted by the manufacturer has identified a high content of protein and moderate quantities of glucosamine (up to 1% by dry weight), chondroitin sulfate (up to 1%), hyaluronic acid (up to 2%), and collagen (Type I, up to 5%).

The multi-center trial reported herein was designed to evaluate the acceptability of this natural arthritis treatment with European orthopedic surgeons and patients. Success of this trial would also

***Corresponding author:** Dr. Ulrich Danesch, Weber & Weber GmbH & Co. KG, Biological Medicinal Products, Herrschinger Str. 33, D-82266 Inning/Ammersee, Germany, Tel: +49-081439270; E-mail: Danesch@weber-weber.net

Received January 24, 2014; **Accepted** July 09, 2014; **Published** July 20, 2014

Citation: Danesch U, Seybold M, Rittinghausen R, Treibel W, Bitterlich N (2014) NEM® Brand Eggshell Membrane Effective in the Treatment of Pain Associated with Knee and Hip Osteoarthritis: Results from a Six Center, Open Label German Clinical Study. J Arthritis 3: 136. doi:10.4172/2167-7921.1000136

validate the extension of the body of clinical evidence for NEM® from the United States to a European population. Therefore, a 2-month open-label study was conducted at six different clinical sites throughout Germany to evaluate the efficacy and tolerability of NEM® for the relief of the pain and discomfort associated with osteoarthritis of the knee and/or hip.

Materials and Methods

Study design

The study was conducted according to a prospective, multi-center, open label design and was conducted in Germany in accordance with the International Conference on Harmonization guideline for the principles of Good Clinical Practice (ICH E6) and the Declaration of Helsinki to ensure protection of human subjects. Patients provided their written informed consent to participate. Neither the clinical investigators nor the patients were blinded to treatment (open label design). Treatment consisted once daily orally of Atrosia® (Weber and Weber, GmbH and Co. KG, Germany) providing 500 mg of NEM® in vegetarian capsules that were stored in closed containers at ambient temperature. Clinic visits were scheduled for subjects at study initiation and at 60 days following the onset of treatment. Treatment compliance was checked at clinic visits by patient interview and by counting the number of unused doses of the study medications. Analgesics (i.e. acetaminophen) were allowed for rescue pain relief. However, subjects recorded the time and amount of analgesic taken in patient diaries so that overall analgesic use could be evaluated as part of the study.

Patients

All subjects 18 years of age or older who were seeking relief of mild to moderate pain due to osteoarthritis of the knee and/or hip were considered for enrollment in the study. In order to be eligible, subjects must have had moderate persistent pain in the knee and/or hip associated with osteoarthritis and must have had baseline scores within the range of 4-7 on the first three questions dealing with joint pain. Subjects that were currently taking analgesic medications or NSAIDs every day, currently taking glucosamine, chondroitin sulfate, MSM, or collagen were ineligible to participate in the study. Patients were excluded if they were currently receiving remission-inducing drugs such as methotrexate or immunosuppressive medications or had received them within the past 3 months. Other exclusionary criteria were: a known allergy to eggs or egg products, or pregnant or breastfeeding women. Subjects participating in any other research study involving an investigational product (drug, device, or biologic) or a new application of an approved product, within 30 days of screening were also excluded from participating in the trials.

Treatment response

The primary outcome measure of this study was to evaluate the mean effectiveness of NEM® in relieving general pain associated with moderate osteoarthritis of the knee and/or hip (Questions 1-9). Additional outcome measures were to evaluate general stiffness (Question 10) and analgesic use during the study. The primary treatment response endpoints were the 10-, 30-, and 60-day patient assessments utilizing a 10-question 'Short Form' questionnaire derived from the Western Ontario and McMasters Universities Osteoarthritis Index questionnaire (WOMAC), which has some precedence [16,17]. Each question included a zero to 10 analog Likert-scale, with zero equating to no pain (or no stiffness) and 10 equating to most severe pain (or most severe stiffness). Patients were asked to mark a number corresponding to the perceived pain (or stiffness) from the affected treatment joint(s). Endpoints were then compared to pretreatment assessments. At the conclusion of the study, subjects were asked to provide a Patient's Global Assessment of treatment efficacy (4 categories-very good/good/moderate/poor) and tolerability (same 4 categories). Clinical investigators were also asked to provide a Physician's Global Assessment of treatment efficacy (5 categories-symptom-free/significant improvement/moderate improvement/unchanged/impaired).

Adverse events

A secondary objective of this study was to evaluate tolerability and any adverse reactions associated with supplementation with NEM®. The subject's self-assessment diaries were reviewed and any discomfort or other adverse events were recorded and reported in accordance with applicable ICH Guidelines. Adverse events and serious adverse events were assessed by the clinical investigator at each study visit and followed until resolution, as necessary. Serious adverse events were required to be reported to the clinical monitor immediately.

Statistical analysis

As this was an open-label study, a simple single group sample size estimate [18] was performed for statistical power determination for a continuous variable. In previous trials with NEM® [6,7], the standard deviation for the study subjects for pain (within the inclusion range of this study) averaged 34.6%. We hoped to be able to detect a 1.5 point difference from baseline within the 10-point Likert scale. Thus a minimum of 43 subjects would need to be enrolled to have a 95% likelihood of detecting the expected improvement with a statistical power of 80%. Comparisons of demographic data from the six clinical sites were made with a Kruskal-Wallis test for multiple independent samples at baseline. Statistical significance was accepted at $p<0.05$. Post-baseline statistical analyses were done as repeated measures Analysis of Variance (rm-ANOVA) with a Greenhouse-Geisser correction. Items found to have statistical significance with rm-ANOVA were then compared using a Wilcoxon test for dependent samples. Statistical significance was accepted at $p<0.05$. Analysis of the primary outcome measure (the change from baseline in general pain levels) was conducted in the per protocol population. SPSS Statistics V19.0 was used for all statistical analyses [19].

Results

Patient recruitment began in March 2012 at six clinical sites in Germany and the final follow-up was conducted in July 2012. A total of forty-four subjects between the ages of 32 and 95 were enrolled with

Age, yrs	67.1 ± 14.0
Sex	
Male (%)	17 (39)
Female (%)	27 (61)
Height, cm	170.2 ± 9.5
Weight, kg	74.2 ± 13.1
Body-mass Index	25.5 ± 4.1
Affected Joint	
Knee (l,r,bilateral)	39 (28,27,16)
Hip (l,r,bilateral)	14 (11,10,7)
Ankle (l,r,bilateral)	3 (2,2,1)

*Except where indicated otherwise, values are reported as mean ± standard deviation (SD) (n=44). BMI was determined as weight in kilograms divided by height in meters squared.

Table 1: Patient Demographics*.

Question 1: *Pain when walking on level ground?*	4.8 ± 1.0
Question 2: *Pain when going up or down stairs?*	5.7 ± 1.0
Question 3: *Pain when at rest (i.e. sitting, lying down, etc.)?*	5.3 ± 1.0
Question 4: *Pain when sitting with legs bent for an extended period of time (i.e. in a car, at a theater, etc.)?*	3.4 ± 1.8
Question 5: *Pain when getting up from a seated position?*	5.3 ± 1.3
Question 6: *Pain when getting in and out of a car, a bathtub, etc.?*	5.3 ± 1.1
Question 7: *Pain when bending, stooping, or kneeling?*	5.7 ± 1.3
Question 8: *Pain when putting on socks or pantyhose?*	4.4 ± 1.9
Question 9: *Pain with light household chores (i.e. laundry, dusting, vacuuming, etc.)?*	4.6 ± 1.7
Question 10: *Stiffness when first getting up from bed in the morning?*	4.2 ± 1.8

*Values are reported as mean ± standard deviation (SD) (n=37)

Table 2: Pooled baseline clinical characteristics for the 10-question patient questionnaire.

	Days Post-treatment	Mean ± SD	Percent Improvement	*P*-value†		Days Post-treatment	Mean ± SD	Percent Improvement	*P*-value†
Question 1	Baseline (n=37)	4.8 ± 1.0	-	-	Question 6	Baseline (n=37)	5.3 ± 1.1	-	-
	10 (n=37)	3.9 ± 1.7	18.1%	0.001*		10 (n=37)	4.4 ± 1.3	15.4%	0.001*
	30 (n=37)	3.3 ± 1.5	30.7%	<0.001*		30 (n=37)	3.7 ± 1.3	29.1%	<0.001*
	60 (n=37)	3.3 ± 1.8	32.4%	<0.001*		60 (n=37)	3.5 ± 1.6	32.8%	<0.001*
Question 2	Baseline (n=37)	5.7 ± 1.0	-	-	Question 7	Baseline (n=37)	5.7 ± 1.3	-	-
	10 (n=37)	4.7 ± 1.7	17.7%	0.001*		10 (n=37)	5.2 ± 1.7	8.6%	0.056
	30 (n=37)	4.1 ± 1.6	26.7%	<0.001*		30 (n=37)	4.4 ± 1.6	22.4%	<0.001*
	60 (n=37)	3.8 ± 1.8	32.6%	<0.001*		60 (n=37)	4.1 ± 1.7	28.0%	<0.001*
Question 3	Baseline (n=37)	5.3 ± 1.0	-	-	Question 8	Baseline (n=37)	4.4 ± 1.9	-	-
	10 (n=37)	4.5 ± 1.5	14.3%	0.001*		10 (n=37)	4.0 ± 1.7	9.2%	0.064
	30 (n=37)	3.8 ± 1.4	27.5%	<0.001*		30 (n=37)	3.2 ± 1.7	25.5%	<0.001*
	60 (n=37)	3.6 ± 1.5	32.6%	<0.001*		60 (n=37)	2.9 ± 1.7	33.6%	<0.001*
Question 4	Baseline (n=37)	3.4 ± 1.8	-	-	Question 9	Baseline (n=37)	4.6 ± 1.7	-	-
	10 (n=37)	2.9 ± 1.9	15.7%	0.042*		10 (n=37)	4.1 ± 1.4	11.7%	0.041*
	30 (n=37)	2.3 ± 1.4	33.8%	<0.001*		30 (n=37)	3.6 ± 1.4	23.0%	0.002*
	60 (n=37)	2.2 ± 2.0	35.6%	<0.001*		60 (n=37)	3.0 ± 1.7	34.9%	<0.001*
Question 5	Baseline (n=37)	5.3 ± 1.3	-	-	Question 10	Baseline (n=37)	4.2 ± 1.8	-	-
	10 (n=37)	4.7 ± 1.6	11.7%	0.012*		10 (n=37)	3.8 ± 1.9	9.9%	0.075
	30 (n=37)	4.0 ± 1.3	24.0%	<0.001*		30 (n=37)	3.0 ± 1.8	27.4%	<0.001*
	60 (n=37)	3.6 ± 2.0	31.7%	<0.001*		60 (n=37)	2.9 ± 1.7	29.3%	<0.001*

†*P*-values were determined by Wilcoxon test for dependent samples following a statistically significant difference as determined by rm-ANOVA, and represent treatment versus baseline. **P*<0.05.

Table 3: Mean values by question in an NEM-supplemented treatment group at baseline and 10, 30 and 60 days post-treatment.

osteoarthritis of the knee and/or hip. Of these subjects, twenty-seven (61%) were female and seventeen (39%) were male. The treated joints consisted of knee (39), hip (14), ankle (3), both either knee and hip (10), or both knee and ankle (2). Of the thirty-nine subjects with knee OA, sixteen (40.0%) had bilateral incidence. Of the fourteen subjects with hip OA, seven (50.0%) had bilateral incidence. Patient demographics are reported in Table **1**. All forty-four subjects completed baseline evaluations. Thirty-seven (84%) of the forty-four subjects completed the two month study per the protocol. Compliance with the study treatment regimen was good.

Patient data was initially evaluated between sites to exclude site bias (not shown). As there were no abnormalities in these evaluations, the data were pooled for all subsequent analyses. A clinical comparison of valid subjects was carried out to obtain a mean baseline score for each of the ten questions from the patient questionnaire (Table 2). Statistical analysis of the primary outcome measure revealed that supplementation with NEM® produced a significant treatment response from baseline at 10 days (Q1-6 and Q9) (8.6% to 18.1% improvement) and at 30 and 60 days for all nine pain-related questions evaluated (22.4% to 35.6% improvement) (Table 3). Treatment response fell just shy of statistical significance at 10 days for Questions 7 and 8 (p=0.056 and p=0.064, respectively). Supplementation with NEM® produced a significant treatment response from baseline at 30 and 60 days for stiffness (Q10) (27.4% to 29.3% improvement). Greater than 59% of patients rated the efficacy of NEM® as good or very good (Table 4) following 60 days of supplementation. Physicians also rated the treatment effective in subjects, with greater than 75% having moderate or significant improvement from baseline after 60 days (Table 5). For the 30 days prior to study commencement, patients consumed on average 7.0 ± 6.0 doses of acetaminophen. Analgesic use had dropped considerably to 2.43 ± 2.69 doses (per 30 days) at 30 days of supplementation with NEM®. Analgesic use rebounded slightly to 3.59 ± 3.86 doses (per 30 days) by the end of the study at day 60. There were two adverse events reported during the study. One was a scratchy throat and was believed to be related to antibiotic use. The other was stomach discomfort which was believed to be related to the study material. There were no serious

Patient's Global Assessment				
	Efficacy		Tolerability	
	Number	Frequency	Number	Frequency
very good	10	27.0%	22	59.5%
good	12	32.4%	10	27.0%
moderate	9	24.3%	2	5.4%
poor	6	16.2%	3	8.1%

Table 4: Patient's Global Assessment of Efficacy and Tolerability following 60 days of NEM® supplementation.

Physician's Global Assessment		
	Treatment response	
	Number	Frequency
symptom-free	0	0.0%
significant improvement	17	45.9%
moderate improvement	11	29.7%
unchanged	9	24.3%
impaired	0	0.0%

Table 5: Physician's Global Assessment of treatment response following 60 days of NEM® supplementation.

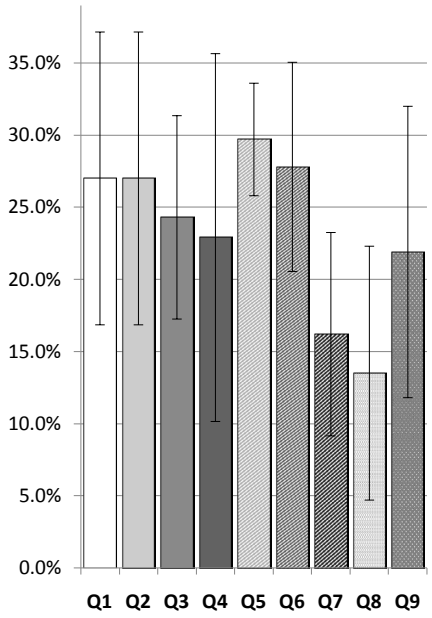

Error bars represent the 95% Confidence Interval for each question.

Figure 1: Percentage of responders achieving 30% improvement in pain-related questions by Day 10.

adverse events reported during the study. The treatment was reported to be well tolerated by study participants with greater than 86% of patients rating NEM® tolerability as good or very good

Discussion

Joint and connective tissue disorders are quite common in Westernized countries [1,20] and result in significant costs, both financial [21] and quality-of-life [22], for those that suffer from the debilitating diseases. This open-label clinical trial was designed to evaluate the acceptability of this natural arthritis treatment with European orthopedic surgeons and patients and to validate the extension of the body of clinical evidence for NEM® from the United States to a European population through the evaluation of the efficacy, safety, and tolerability of NEM® brand eggshell membrane as a treatment option for osteoarthritis of the knee and/or hip. Results of the study indeed suggest that NEM® is both effective and safe for treating pain associated with osteoarthritis of the knee and/or hip in a European population.

Patients experienced relatively rapid (10 days) responses for pain-related questions with a mean response of approximately 14%. By the end of the follow-up period (60 days) the mean response for pain-related questions had more than doubled to approximately 33%. A brief responder analysis of the data provides a number of clinically relevant highlights. On average, nearly 1/4th of the subjects experienced a 30% improvement in pain-related questions within 10 days (Figure 1). And almost 20% of the study population experienced a 50% improvement in pain-related questions by the end of the study (60 days) (not shown). These results align well with results from previous clinical studies of NEM® that were conducted in the U.S. [6,7].

The safety profile for NEM® is also of significance as this is the fifth clinical trial to date in which there have been no reports of serious adverse events associated with treatment. No side effects from consuming NEM® have thus far been identified, excluding the obvious egg allergy concern. This is of obvious importance in a condition such as osteoarthritis that requires long-term treatment.

The trial had a limited initial enrollment (44 subjects), however there was a relatively low drop-out rate (16%) and good treatment compliance. As the trial was also open label, there is the obvious issue of the placebo effect. The inclusion of a placebo control would have provided greater clinical meaning, however it would have required a significantly larger study population.

Conclusions

With so many people suffering from osteoarthritis of the knee and hip in Western populations, it is important for patients to have treatment options that are both safe and effective. The reporting of the results from this six center, open label German clinical study demonstrates that NEM® brand eggshell membrane may be a viable treatment option for the management of osteoarthritis of the knee and/or hip in the broader European population. In this clinical study, NEM®, 500 mg taken once daily, significantly reduced pain, both rapidly (10 days) and continuously (60 days). It also showed clinically meaningful results from a brief responder analysis, demonstrating that a significant proportion of treated patients will benefit from NEM® supplementation.

Acknowledgement

The study sponsor was Weber and Weber GmbH and Co. KG. UD, MS and RR are employed by the sponsor. WT and NB have no competing interests. The authors would like to acknowledge ESM Technologies, LLC for providing the powdered NEM® ingredient used to produce the study capsules for this trial.

References

1. Quintana JM, Arostegui I, Escobar A, Azkarate J, Geonaga I, et al (2008) Prevalence of Knee and Hip Osteoarthritis and the Appropriateness of Joint Replacement in an Older Population. Arch Intern Med 168(14): 1576-1584.
2. Altman RD (1999) Ibuprofen, acetaminophen and placebo in osteoarthritis of the knee: a six-day double-blind study. Arthritis Rheum 42(S403).
3. Case JP, Baliunas AJ, Block JA (2003) Lack of Efficacy of Acetaminophen in Treating Symptomatic Knee Osteoarthritis. Arch Intern Med 163: 169-178.
4. Geba GP, Weaver AL, Polis AB, Dixon ME, Schnitzer TJ (2002) Efficacy of

Rofecoxib, Celecoxib, and Acetaminophen in Osteoarthritis of the Knee. J Am Med Assoc 287: 64-71.

5. Towheed TE, Maxwell L, Judd MG, Catton M, Hochberg MC, Wells G (2006) Acetaminophen for osteoarthritis. Cochrane Database of Systematic Reviews 1: CD004257.
6. Ruff KJ, Winkler A, Jackson RW, DeVore DP, Ritz BW (2009) Eggshell membrane in the treatment of pain and stiffness from osteoarthritis of the knee: a randomized, multicenter, double-blind, placebo-controlled clinical study. Clin Rheumatol 28: 907-914.
7. Ruff KJ, DeVore DP, Leu MD, Robinson MA (2009) Eggshell membrane: A possible new natural therapeutic for joint and connective tissue disorders. Results from two open-label human clinical studies.ClinInterv Aging 4: 235-240.
8. Wong M, Hendrix MJC, von der Mark K, Little C, Stern R (1984) Collagen in the egg shell membranes of the hen. Dev Biol 104: 28-36.
9. Baker JR, Balch DA (1962) A study of the organic material of hen's-egg shell. Biochem J 82: 352-361.
10. Long FD, Adams RG, DeVore DP (2005) Inventors. Preparation of hyaluronic acid from eggshell membrane. U.S. Patent No. 6,946,551.
11. Ha YW, Son MJ, Yun KS, Kim YS (2007) Relationship between eggshell strength and keratan sulfate of eggshell membranes. Comp BiochemPhysiol A MolIntegr Physiol 147: 1109-1115.
12. Richy F, Bruyere O, Ethgen O, Cucherat M, Henrotin Y, Reginster JY (2003) Structural and Symptomatic Efficacy of Glucosamine and Chondroitin in Knee Osteoarthritis: A Comprehensive Meta-analysis. Arch Intern Med 163: 1514-1522.
13. Moreland LW (2003) Intra-articular hyaluronan (hyaluronic acid) and hylans for the treatment of osteoarthritis: mechanisms of action. Arthritis Res Ther 5: 54-67.
14. Benson KF, Ruff KJ, Jensen GS (2012) Effects of Natural Eggshell Membrane (NEM) on Cytokine Production in Cultures of Peripheral Blood Mononuclear Cells: Increased Suppression of Tumor Necrosis Factor-α Levels After In Vitro Digestion. J Med Food 15: 360-368.
15. Ruff KJ, DeVore DP (2014) Reduction of pro-inflammatory cytokines in rats following 7-day oral supplementation with a proprietary eggshell membrane-derived product. Mod Res Inflamm 3: 19-25.
16. Baron G, Tubach F, Ravaud P, Logeart I, Dougados M (2007) Validation of a Short Form of the Western Ontario and McMasters Universities Osteoarthritis Index Function Subscale in Hip and Knee Osteoarthritis. Arthritis Rheum 57(4): 633-638.
17. Bilbao A, Quintana JM, Escobar A, Las Hayas C, Orive M (2011) Validation of a proposed WOMAC short form for patients with hip osteoarthritis. Health Qual Life Outcome 9: 75.
18. National Research Council (2003)Guidelines for the Care and Use of Mammals in Neuroscience and Behavioral Research.The National Academies Press Washington, DC.
19. IBM Corporation. SPSS Statistics.
20. Helmick CG, Felson DT, Lawrence RC, Gabriel S, Hirsch R, et al (2008) Estimates of the Prevalence of Arthritis and Other Rheumatic Conditions in the United States. Part I. Arthritis Rheum 58: 15-25.
21. U.S. Centers for Disease Control (2007) National and state medical expenditures and lost earnings attributable to arthritis and other rheumatic conditions -United States, 2003. Morbidity and Mortality Weekly Report 56: 4-7.
22. Cook C, Pietrobon R, Hegedus E (2007) Osteoarthritis and the impact on quality of life health indicators. Rheumatol Int 27: 315-321.

Citation: Danesch U, Seybold M, Rittinghausen R, Treibel W, Bitterlich N (2014) NEM® Brand Eggshell Membrane Effective in the Treatment of Pain Associated with Knee and Hip Osteoarthritis: Results from a Six Center, Open Label German Clinical Study. J Arthritis 3: 136. doi:10.4172/2167-7921.1000136

JOURNAL OF MEDICINAL FOOD
J Med Food 15 (4) 2012, 360–368

DOI: 10.1089/jmf.2011.0197

Effects of Natural Eggshell Membrane (NEM) on Cytokine Production in Cultures of Peripheral Blood Mononuclear Cells: Increased Suppression of Tumor Necrosis Factor-α Levels After *In Vitro* Digestion

Kathleen F. Benson,[1] Kevin J. Ruff,[2] and Gitte S. Jensen[1]

[1]*NIS Labs, Klamath Falls, Oregon, USA.*
[2]*ESM Technologies, LLC, Carthage, Missouri, USA.*

ABSTRACT Tumor necrosis factor-α (TNF-α) plays an important role in inflammatory processes. This study examined the effects of natural eggshell membrane (NEM®) (ESM Technologies, LLC, Carthage, MO, USA) on interleukin (IL)-2, IL-4, IL-6, IL-10, interferon-γ (IFN-γ), and TNF-α cytokine production by 4-day peripheral blood mononuclear cell (PBMC) cultures exposed to serial dilutions of either an aqueous extract of natural eggshell membrane (NEM-AQ) or NEM subjected to *in vitro* digestion (NEM-IVD). The effects on cytokine production were also assessed in the presence of phytohemagglutinin (PHA) and pokeweed mitogen (PWM) where exposure to NEM-AQ resulted in reduced levels of proliferation and statistically significant effects on IL-6, IL-10, IFN-γ, and TNF-α cytokine production. NEM-AQ reduced levels of IL-6, IL-10, IFN-γ, and TNF-α in cultures exposed to PHA. In cultures containing PWM, NEM-AQ reduced production of IL-10 and at the highest dose tested increased IL-6 and decreased TNF-α cytokine levels. NEM-IVD, at the two lowest concentrations of product, significantly reduced TNF-α production by PBMC cultures exposed to PWM compared with the *in vitro* digest control or native NEM. Taken together, these results suggest that NEM-AQ can influence signaling events in response to the T cell-specific mitogen PHA as well as to the mitogen PWM that require cellular cross-talk and that these effects may be partially mediated through a reduction in level of the pro-inflammatory cytokine TNF-α. The suppression of TNF-α production in the presence of NEM-IVD is promising for the use of NEM as a consumable anti-inflammatory product.

KEY WORDS: • *cytokines* • *human* • *immunity* • **in vitro** *digestion* • *lymphocyte* • *natural eggshell membrane* • *natural product* • *peripheral blood mononuclear cells* • *Th1/Th2* • *tumor necrosis factor-α*

INTRODUCTION

THE MAIN CLINICAL MANIFESTATIONS of arthritis are inflammation, pain, and bone resorption. Chronic inflammation and bone loss are closely linked pathophysiologic events. New scientific data point to a beneficial effect of blocking specific molecular interactions, which can reduce local arthritic symptoms even in the presence of ongoing chronic inflammation.[1] The current mainstream medical treatments for arthritis involve pain management, anti-inflammatory drugs (nonsteroidal anti-inflammatory drugs, steroids, cyclooxygenase-2 inhibitors), and also exploration of chemokine receptor antagonists to stop cell migration into the inflamed areas.[2–4] Part of the intensive pharmaceutical research efforts includes research on the interaction between osteoblasts and osteoclasts via the receptor activator of nuclear factor κB and its ligand. Receptor activator of nuclear factor κ is a hematopoietic surface receptor controlling osteoclastogenesis and calcium metabolism. Interference with these various pathways may also include arresting the maturation of phagocytic mononuclear cells into bone-resorbing cells, neutralizing pro-inflammatory cytokines, and blocking of matrix metalloproteinases. These mainstream treatments go far beyond a direct treatment of cells within the arthritic joints. They aim at reducing inflammation and inhibiting recruitment into the inflamed area of cells that contribute to disease processes, including bone resorption.

In contrast, nutraceutical products widely used for joint health include glucosamine, chondroitin, and hyaluronic acid, thus ignoring a multifaceted action of complex natural products. Even the spotlight on hyaluronic acid seems to limit its focus on replenishing the synovial fluid and on stimulating chondrocytes to produce more hyaluronic acid, thus ignoring the many complex ways that hyaluronic acid can modulate cells and their behavior.

Natural eggshell membrane (NEM®) (ESM Technologies, LLC, Carthage, MO, USA) is a novel dietary supplement that has been shown in several human trials to be a clinically effective treatment for pain and stiffness associated with joint and connective tissue disorders, particularly osteoarthritis.[5,6] Eggshell membrane is primarily composed

Manuscript received 26 December 2010. Revision accepted 10 October 2011.

Address correspondence to: Gitte S. Jensen, NIS Labs, 1437 Esplanade, Klamath Falls, OR 97601, USA, E-mail: gitte@nislabs.com

of fibrous proteins such as collagen type I.[7] However, eggshell membranes have also been shown to contain glycosaminoglycans, such as dermatan sulfate, chondroitin sulfate,[8] and hyaluronic acid,[9] and sulfated glycoproteins, including hexosamines such as glucosamine.[10] NEM contains up to about 5% of these various components, the unique combination of which may explain its biological activity. To further this understanding, a cytokine profile was determined from NEM-treated lymphocytes in cell culture.

The purpose of this study is to evaluate anti-inflammatory and immunomodulatory effects of NEM as well as its *in vitro* digest in a select series of human cell-based *in vitro* assays, in preparation for more comprehensive evaluations *in vitro* and *in vivo*.

MATERIALS AND METHODS

Reagents

Phosphate-buffered saline (PBS) (pH 7.4), RPMI-1640 culture medium, fetal calf serum, L-glutamine (200 m*M*), penicillin–streptomycin (100× solution), glacial acetic acid, methanol, pepsin, pancreatin, bile salts, Histopaque 1077, and Histopaque 1119 were obtained from Sigma-Aldrich (St. Louis, MO, USA). The cytometric bead array (CBA) for human Th1/Th2 cytokine kit II was purchased from BD Biosciences (San Jose, CA, USA). All reagents for sodium dodecyl sulfate (SDS)–polyacrylamide gel electrophoresis (PAGE) and silver stain detection were obtained from Bio-Rad (Hercules, CA, USA) and included 4–15% Tris-HCl ready gels, Precision Plus dual color protein molecular weight standards, Laemmli buffer, 10×Tris/glycine/SDS buffer, silver stain concentrate, silver stain oxidizer, and silver stain developer. NEM was obtained from ESM Technologies, LLC.

Preparation of NEM for in vitro *bioassays*

The NEM powder was reconstituted in physiological saline and allowed to rehydrate for 1 hour at room temperature. Solids included insoluble calcium carbonate from eggshell and were removed by centrifugation at 900 *g* for 10 minutes. The liquid was filtered through a sterile cellulose acetate syringe filter (pore size, 0.22 μm). This filtrate corresponded to a stock solution of 100 g/L product (same concentration as the *in vitro*–digested NEM [NEM-IVD], described below). This aqueous preparation is designated NEM-AQ.

Preparation of an in vitro *digest of NEM*

The *in vitro* digestion of NEM was performed according to methods published in the literature[11–13] (see also Fig. 4). In brief, 3.75 g of NEM powder was added to 30 mL of PBS and shaken at room temperature for 1 hour. Following the 1-hour incubation, the sample was spun at 900 *g* for 10 minutes, and the aqueous solution was removed from the solids and sterile-filtered with a cellulose acetate filter (pore size, 0.22 μm). HCl (1 *M*) was then added until the solution reached pH 2.0. Porcine pepsin was then added at a concentration of 1.3 mg/mL, and the sample was left at 37°C for 60 minutes with shaking (to simulate digestion in the stomach). Next, sodium bicarbonate ($NaHCO_3$) was used to increase the pH of the solution to 5.8 (irreversibly inactivating pepsin), and pancreatin (0.175 mg/mL) and porcine bile salts (1.1 mg/mL) were added to simulate intestinal digestion. The pH was then adjusted to 6.5, and the mixture was left at 37°C for 1 hour. The final volume of the digest was adjusted with saline to give a final concentration of NEM of 100 g/L. Following this *in vitro* digestion, the sample was centrifuged through a 10-kDa cutoff filtration spin column to remove the enzymes from the digested product. This filtration step was necessary to avoid the presence of digestive enzymes in the downstream treatment of cells with product. This step also avoided the use of enzyme inhibitors that potentially could have direct effects on cell signaling in downstream cell-based assays. The liquid after *in vitro* digestion and size-exclusion filtration is designated NEM-IVD.

As the control, saline alone (negative control) was simultaneously subjected to the *in vitro* digestion protocol as described above. This was an important control to determine whether any bile salts or breakdown products from the enzymes themselves have biological activity. This PBS control is designated as PBS-IVD.

SDS-PAGE

SDS-PAGE was performed to compare crude NEM-AQ, NEM-IVD, and the PBS-IVD control. Samples were denatured by boiling for 3 minutes in 1×Laemmli buffer and separated by gel electrophoresis through a 4–15% polyacrylamide Tris-HCl gel using Protein Plus dual color molecular weight standards for reference. Silver staining was performed in order to visualize proteins, and an image of the stained gel was captured with a Canon (Lake Success, NY, USA) PowerShot SD430 digital camera.

Purification of peripheral blood mononuclear cells

Healthy human volunteers between the ages of 20 and 50 years served as blood donors after written informed consent was obtained, as approved by the Sky Lakes Medical (Klamath Falls, OR, USA) Center Institutional Review Board. Isolation of peripheral blood mononuclear cells (PBMCs) was performed as previously described.[14] PBMCs were used to establish lymphocyte cultures for the measurement of cytokine production.

Cytokine production by 4-day PBMC cultures

Freshly purified PBMCs were resuspended in RPMI 1640 medium supplemented with 10% fetal bovine serum, L-glutamine (2 m*M*), penicillin (100 U/mL), and streptomycin (100 mg/mL) at a density of 1×10^6/mL. Cells were cultured in the presence of 10-fold serial dilutions of NEM-AQ, NEM-IVD, or PBS-IVD in a series of triplicate wells containing a total volume of 200 μL. Three separate sets of

culture conditions were established: no mitogen, phytohemagglutinin (PHA), or pokeweed mitogen (PWM). The culture plate was incubated at 37°C in an atmosphere of 5% CO_2 for 4 days, after which cells were transferred to a V-bottom plate and centrifuged. Cell supernatants were collected for cytokine measurement (described below). Determination of relative cell numbers in each culture well was performed by staining cells with the DNA dye CyQuant® (Invitrogen, Carlsbad, CA, USA) and measuring fluorescence measured with a Tecan (Durham, NC, USA) Spectrafluor fluorescence plate reader. Samples were assayed in triplicate, and experiments were repeated three times with cells from three different donors.

Th1/Th2 cytokine profile

The cytokines interleukin (IL)-2, IL-4, IL-6, IL-10, tumor necrosis factor-α (TNF-α), and interferon-γ (IFN-γ) were quantified in the 4-day PBMC culture supernatants using a flow cytometry cytometric bead array (CBA) kit (CBA human Th1/Th2 cytokine kit II, BD Biosciences) that allowed the determination of the levels of all six cytokines simultaneously. Samples were tested in duplicate following the manufacturer's instructions, data were acquired with a FACSCalibur™ flow cytometer (Becton-Dickinson, San Jose), and the analysis was performed with FlowJo software (TreeStar Inc., Ashland, OR, USA).

Statistical analysis

Statistical significance was tested using Student's *t* test performed with the program Microsoft (Redmond, WA, USA) Excel. All *P* values were two-sided and were considered significant when $P < .05$. Only statistically significant *P* values are reported.

RESULTS

Lymphocyte proliferation assay

The lymphocyte proliferation assay evaluates whether a test product alters lymphocyte responsiveness to known signals such as mitogens. If any change in the proliferative response to known mitogens is seen in cells pretreated with test product, this is a good indication that the product has immunomodulatory effects and justifies further in-depth work on T and B lymphocyte signaling and activation.

Freshly purified human PBMCs were cultured for 4 days in the absence versus presence of serial dilutions of test products. Three parallel sets of cultures were established, where one tested the direct effect of test product on lymphocyte proliferation, and the two others examined the possible interference with response to the mitogen PHA or PWM. PHA produces a cleaner signal as it strictly induces proliferation of T lymphocytes, but PWM represents a more physiological signal mimicking the cellular interactions between monocytes/macrophages and T and B lymphocytes that occur in lymphoid tissue; therefore it is beneficial to test both in parallel. Positive controls included cells treated only with a mitogen in the absence of test product. No direct effects of product on lymphocyte proliferation were observed (data not shown). In the presence of PHA (Fig. 1A) and PWM (Fig. 1B), statistically significant decreases in proliferation of 30% and 15%, respectively, were seen with all three dilutions of NEM-AQ, indicating that pretreatment of PBMCs with NEM-AQ altered their response to subsequent signals.

Changes in Th1/Th2 cytokine levels

Supernatants were collected from 4-day cultures where PBMCs were exposed to test products in the absence versus presence of the mitogens PHA and PWM and analyzed for

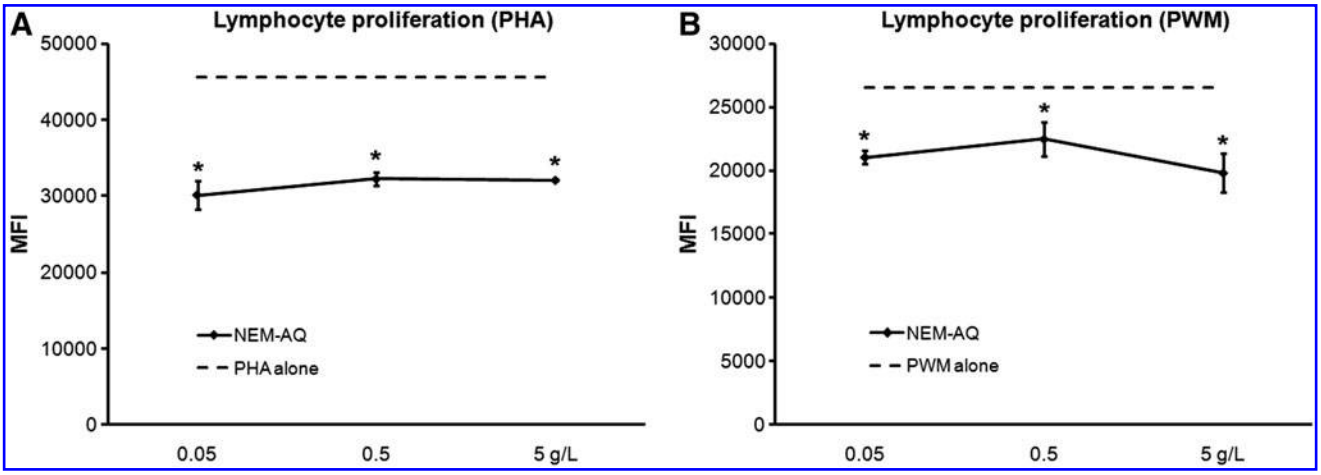

FIG. 1. Effect of aqueous extract of Natural Eggshell Membrane (NEM) (NEM-AQ) on lymphocyte proliferation in the presence of **(A)** phytohemagglutinin (PHA) and **(B)** pokeweed mitogen (PWM). Statistically significant decreases in the proliferative response of 4-day lymphocyte cultures to **(A)** PHA and **(B)** PWM were seen when cells were exposed to serial dilutions of NEM-AQ. Statistically significant differences are indicated ($*P < .05$). Conditions were assayed in triplicate, and the results shown are mean ± SD values from a representative of three separate experiments using cells from three different donors. MFI, mean fluorescence intensity.

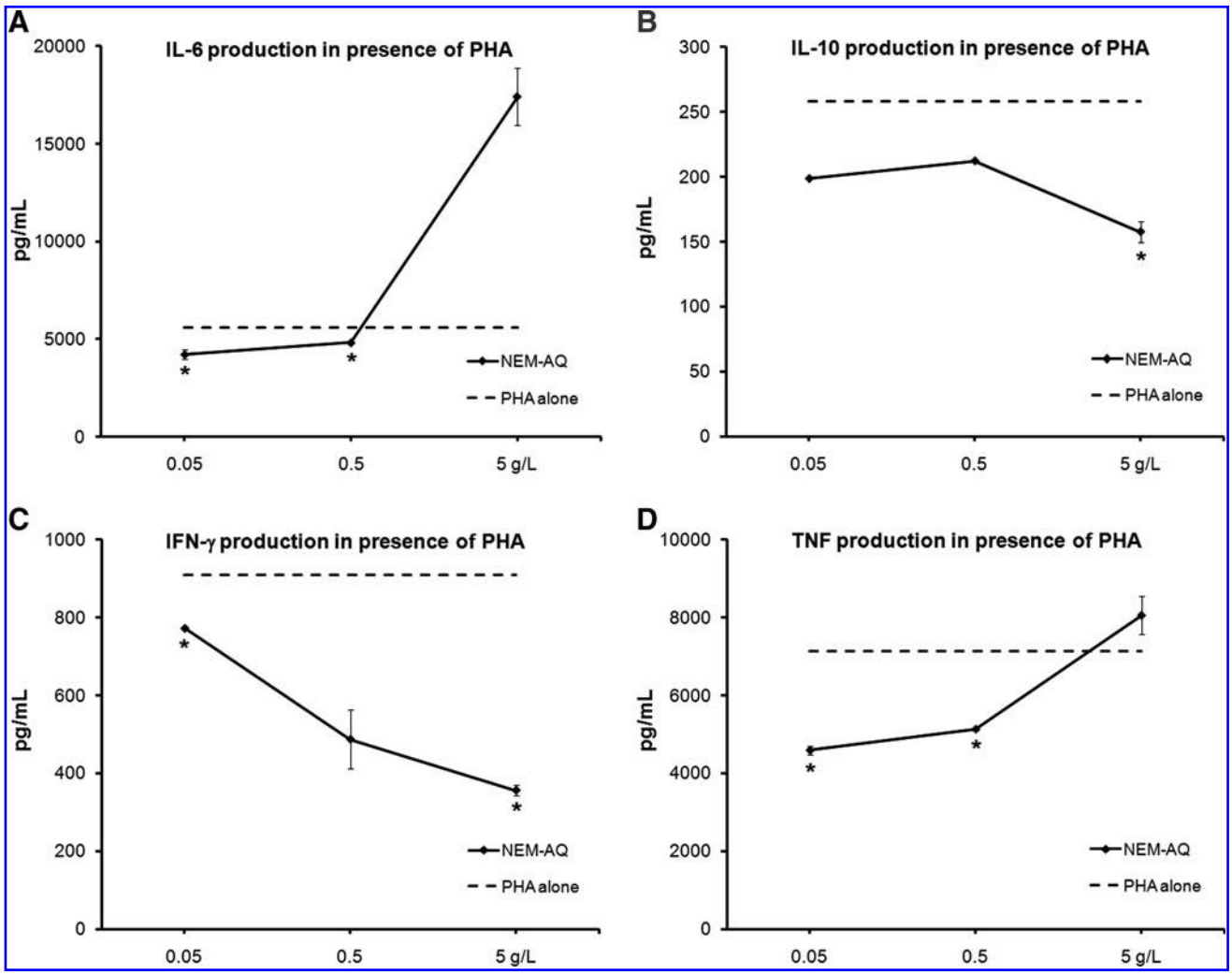

FIG. 2. Effects of NEM-AQ on production of the cytokines **(A)** interleukin (IL)-6, **(B)** IL-10, **(C)** interferon-γ (IFN-γ), and **(D)** tumor necrosis factor-α (TNF-α) by 4-day peripheral blood mononuclear cell cultures simultaneously exposed to PHA. Supernatants from 4-day peripheral blood mononuclear cell cultures were simultaneously assayed for the presence of the cytokines IL-6, IL-10, IFN-γ, and TNF-α using a flow cytometry–based assay. **(A)** IL-6 production in cultures exposed to serial dilutions of NEM-AQ showed a strong increase at the highest dose tested (5 g/L) and a decrease at the two lowest concentrations of NEM-AQ tested. **(B)** Decreases in IL-10 production were seen with all three doses of NEM-AQ in the presence of PHA. **(C)** The cytokine IFN-γ levels decreased in a dose-dependent manner. This reduction in IFN-γ production was over 60% at the highest concentration of NEM-AQ tested. **(D)** TNF-α production decreased in cultures exposed to serial dilutions of NEM-AQ. Statistically significant differences are indicated ($^*P < .05$). The results shown are mean ± SD values from a representative of three separate lymphocyte proliferation cultures using cells from three different donors.

the panel of Th1/Th2 cytokines IL-2, IL-4, Il-6, IL-10, IFN-γ, and TNF-α, using a CBA for flow cytometry. No statistically significant changes in cytokine production occurred in unstimulated cultures, whereas statistically significant changes in the cytokines IL-6, IL-10, IFN-γ, and TNF-α occurred in cultures that contained PHA (Fig. 2) or PWM (Fig. 3).

Cultures exposed to serial dilutions of NEM-AQ showed a biphasic response, including a strong increase of IL-6 at the highest dose tested (5 g/L) in the presence of both PHA and PWM, a decrease at the lower concentrations for PHA, and no effect at lower doses for PWM. Levels of IL-10, IFN-γ, and TNF-α decreased in the presence of all three doses of NEM-AQ in the presence of PHA. Effects in the presence of PWM were only seen at higher doses. The reduction in IFN-γ production in the presence of PHA was over 60% at the highest concentration of NEM-AQ tested. At the 0.05 g/L dose, a 35% reduction in TNF-α levels was seen, indicating a strong anti-inflammatory effect of NEM-AQ on TNF-α production at lower concentrations in the presence of the T-cell mitogen PHA.

In vitro *digest*

An *in vitro* digest as outlined in Figure 4 was performed on NEM-AQ as well as a saline control (PBS-IVD), and the resulting material was subjected to SDS-PAGE and silver stain detection in parallel with NEM-AQ. This analysis

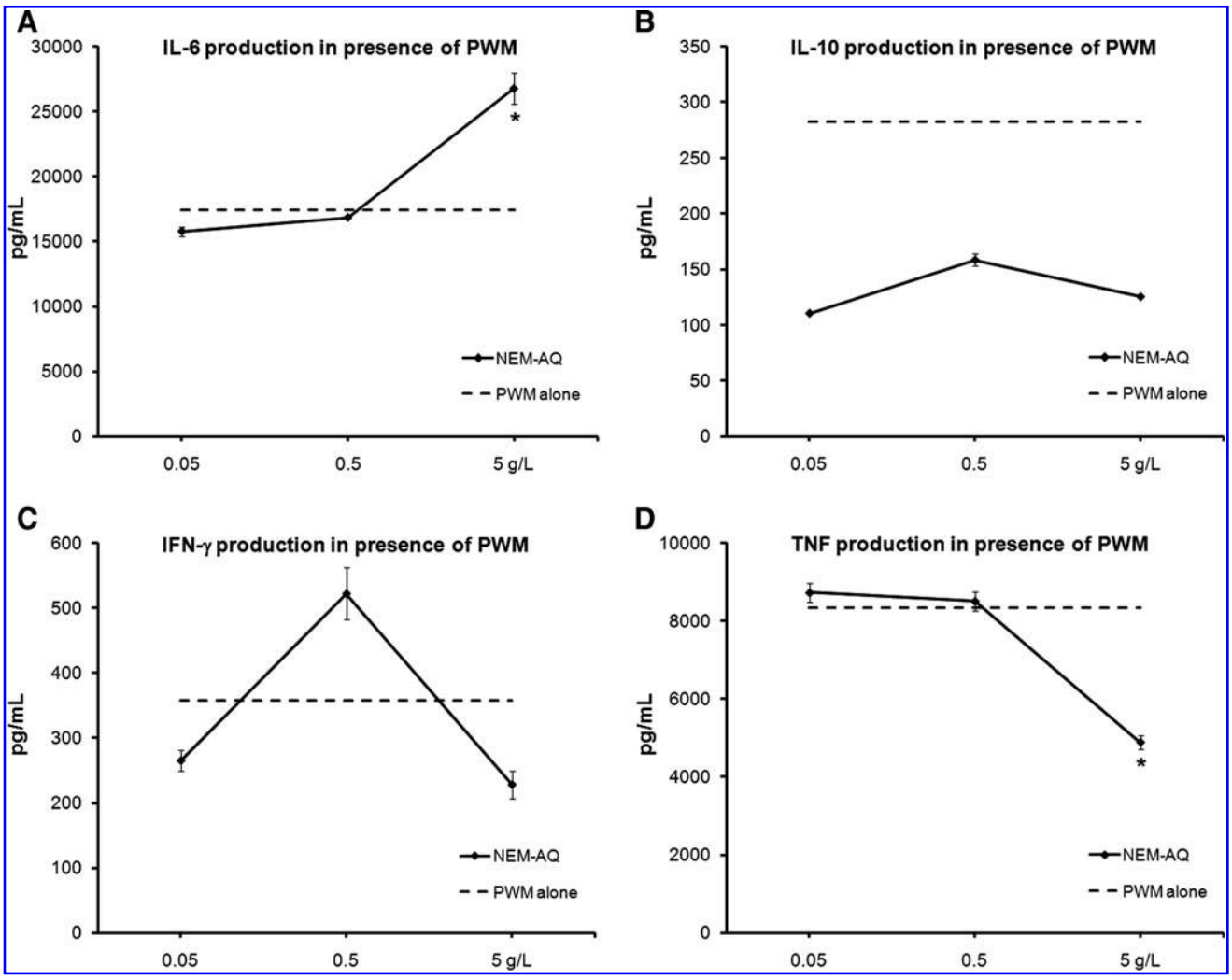

FIG. 3. Effects of NEM-AQ on production of the cytokines **(A)** IL-6, **(B)** IL-10, **(C)** IFN-γ, and **(D)** TNF-α by 4-day peripheral blood mononuclear cell cultures simultaneously exposed to PWM. Supernatants from 4-day peripheral blood mononuclear cell cultures were simultaneously assayed for the presence of cytokines using a flow cytometry–based assay. **(A)** IL-6 production in cultures exposed to serial dilutions of NEM-AQ showed a strong increase at the highest dose tested (5 g/L), whereas lower concentrations of NEM-AQ had no effect compared with IL-6 production in cultures exposed to PWM alone. **(B)** All three concentrations of NEM-AQ decreased IL-10 production in the presence of PWM about twofold. **(C)** Production of IFN-γ by 4-day cultures exposed to serial dilutions of NEM-AQ in the presence of PWM was affected differently depending on the concentration of NEM-AQ. These changes were not statistically significant. **(D)** In the presence of PWM, TNF-α production by 4-day cultures was decreased by the highest concentration of NEM-AQ, whereas lower concentrations of NEM-AQ had no effect on TNF-α production. Statistically significant differences are indicated ($*P < .05$). The results shown are mean ± SD values from a representative of three separate lymphocyte proliferation cultures using cells from three different donors.

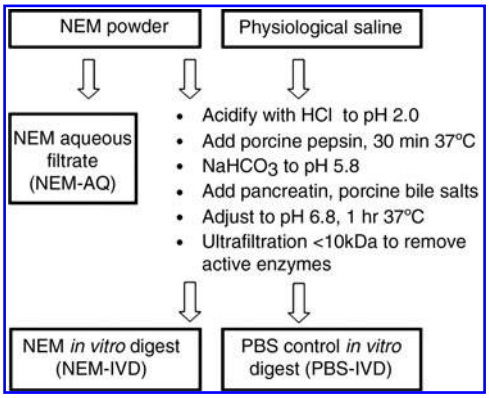

FIG. 4. Diagram outlining the *in vitro* digestion procedure. Based on methods published in the literature,[11–13] a stepwise process was performed that incorporated digestive enzymes derived from pig (porcine) and pH adjustments in order to mimic the digestive processes occurring in the stomach and small intestine. The final digested product was returned to physiological pH and subjected to size-exclusion centrifugation using a 10-kDa filtration column in order to remove the porcine enzymes. This process was performed with NEM-AQ, resulting in the product referred to as *in vitro*–digested NEM (NEM-IVD), as well as with phosphate-buffered saline (PBS), resulting in the product referred to as PBS-IVD.

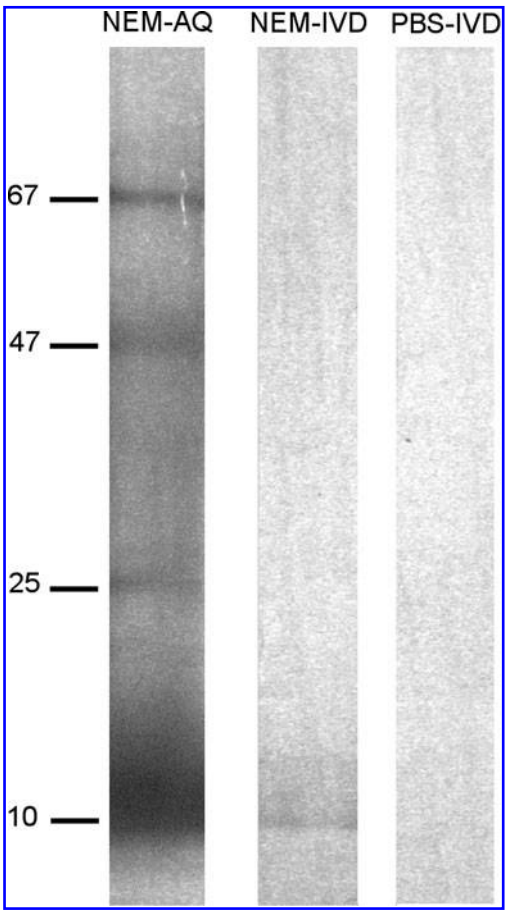

FIG. 5. Sodium dodecyl sulfate–polyacrylamide gel electrophoresis separation of NEM-AQ, NEM-IVD and PBS-IVD. Samples were separated on a 4–15% polyacrylamide gel using denaturing conditions, and bands were visualized by silver stain. Molecular sizes of major bands in the NEM-AQ lane are indicated in kDa on the left-hand side. This presentation of the data is used to show the effects of the *in vitro* digestion of NEM on the molecular weights of the resulting digested protein products. This comparison shows a loss of higher-molecular-weight products when comparing NEM-IVD with the undigested NEM-AQ. Within the sensitivity of sodium dodecyl sulfate–polyacrylamide gel electrophoresis and silver stain methods, no residual enzymes or breakdown products from the *in vitro* digestion process were detectable in the PBS-IVD sample.

showed a reduction of high-molecular-weight material in the NEM-IVD sample (Fig. 5) compared with the NEM-AQ sample, whereas the PBS-IVD sample did not show any detectable protein.

Suppression of TNF-α production resulting from treatment of PBMCs with NEM-IVD

In the context of the mitogen PWM, reflecting an *in vitro* model of the cellular collaborations in lymphoid tissue, the native NEM-AQ showed an anti-inflammatory effect only at the highest dose used, and the effect returned to baseline at the lower doses. In contrast, NEM-IVD showed significant anti-inflammatory properties across a wide dose range with

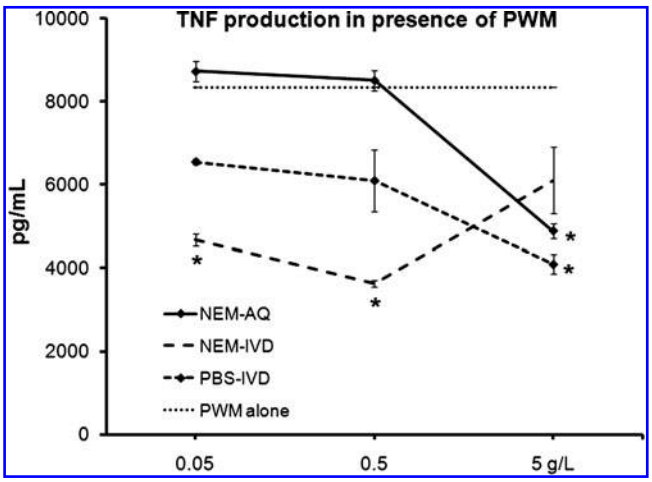

FIG. 6. Comparison of the effect of NEM-AQ, NEM-IVD, and PBS-IVD on production of the cytokine TNF-α by 4-day peripheral blood mononuclear cell cultures simultaneously exposed to PWM. TNF-α production by cultures exposed to PWM was most affected by the NEM-IVD extract. At the highest dose of extracts tested (5 g/L), all three products produced a similar reduction in TNF-α production of 30–40%. However, it can be argued that this high dose is beyond a physiological relevant dose after consumption. Therefore, the data for the two lower doses may be more relevant for predicting *in vivo* outcomes. At the two lowest doses of extracts tested, a different picture emerged. Here NEM-AQ did not affect TNF-α production, showing cytokine levels similar to baseline (cultures exposed to PWM alone). The PBS-IVD extract showed some activity, lowering TNF-α production. However, NEM-IVD had the greatest effect in lowering TNF-α production. At the 0.5 and 0.05 g/L concentrations, NEM-IVD lowered TNF-α production by 55% and 45%, respectively. Statistically significant differences are indicated (*$P < .05$). The results shown are mean ± SD values from a representative of three separate lymphocyte proliferation cultures using cells from three different donors.

respect to TNF-α production (Fig. 6). The *in vitro*–digested saline control (PBS-IVD) had some effects on PBMC culture proliferation and cytokine production that were different from those of saline alone, suggesting the presence of residual material derived from the *in vitro* digestion process. The effects seen at the two lower doses may be most relevant for predicting *in vivo* outcomes. The data showed that in the presence of PWM, NEM-AQ had only a minor effect on TNF-α production, whereas NEM-IVD showed 45–55% suppression of TNF-α production ($P < .04$).

DISCUSSION

Osteoarthritis is often considered a local problem centered on the specific target area where bone and joint degradation is seen, such as, for example, a knee. However, osteoarthritis is a systemic disease, involving immune dysregulation and altered cytokine profile (Fig. 7). In particular, T cells likely play an important role in the pathogenesis and progression of osteoarthritis. Osteoarthritis involves infiltrating monocytes producing TNF-α.[15] It is also believed that peripheral blood leukocytes, which travel through the tissues of inflamed joints, are activated

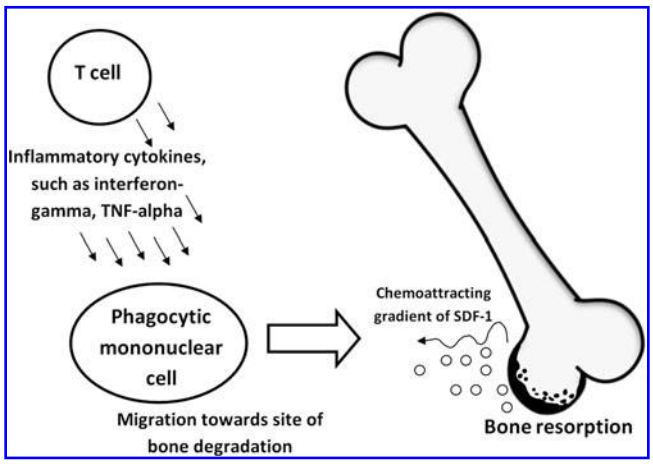

FIG. 7. Diagram showing arthritic mechanisms of action involving T-cell–derived inflammatory cytokines in activation and migration of phagocytic mononuclear cells into areas of bone destruction. SDF-1, stromal cell–derived factor-1.

through exposure to locally produced mediators of inflammation (*i.e.*, IL-1β, TNF-α, etc.).[16] We were therefore interested in studying cytokine production in peripheral blood mixed cultures including monocytes. This was accomplished through an extended proliferation/cytokine assay, where both digested and undigested NEM preparations with appropriate controls were tested in serial dilutions in the presence and absence of mitogens. Two mitogens were tested in parallel: PHA, which is a T-cell mitogen that will induce T-cell proliferation, and PWM, which is a mitogen that requires the collaboration of T cells, B cells, and monocytes in the culture.

The significance of the data must be interpreted in light of the specificity of the culture conditions in the presence of the two separate mitogens, PHA and PWM, as well as the importance of the sequence in which stimulating agents were added. PWM is an aqueous extract from *Phytolacca americana* (pokeweed) that has mitogenic properties that involve mechanisms closely mimicking events in lymph nodes and other immune tissue where antigen presentation leads to co-stimulation and collaboration of multiple cell subsets. The mechanisms involve leukocyte aggregation.[17] RNA synthesis precedes DNA synthesis by 24 hours, after which cell division begins, involving up to 60% of the peripheral blood lymphocyte fraction.[18] The activation process involves T lymphocytes, B lymphocytes, and phagocytic mononuclear cells[19] in tandem and generates both T cell– and B cell–derived cytokines,[20] leading to generation of immunoglobulin-secreting plasma cells[21] and a shift in CD45 isoform expression indicative of plasma cell differentiation.[22] In contrast, an extract from *Phaseolus vulgaris* (red kidney bean) called PHA predominantly activates T lymphocytes, even though some B-cell activation can be seen as a result of the activated T cells triggering some B lymphocytes into proliferation.[23] Therefore, these two mitogens were used as a method to shed light on events that are strictly T cell mediated versus events that require complex cellular collaboration (B cells and T cells).

The reduction of proliferation in NEM-treated cultures should not be seen as a suppression of a mitogenic response, but rather as evidence that NEM has leukocyte signaling properties of its own. The sequential addition of NEM first, followed by mitogens after 5 minutes, allowed compounds in NEM to engage signaling in target cells so when the mitogens were subsequently added the resultant signal was diminished.

Because NEM affected both PHA and PWM mitogenicity, but in different ways, this finding suggests specific mechanisms, including that NEM contains compounds directly able to modulate T-cell activation, and that NEM also has immune-modulating properties in the context of a more physiological activation process, such as in the PWM model of lymphocyte activation.

Cytokine production was affected in the cultures, with significant changes in three inflammatory cytokines: IL-6, IFN-γ, and TNF-α. It is interesting that this did not change when NEM was passed through the *in vitro* digestion protocol, except for TNF-α. The reduction in TNF-α production with NEM-IVD was seen at 100-fold lower doses than with undigested NEM. In the case of PWM stimulation, NEM-IVD showed anti-inflammatory properties by drastically reducing the production of TNF-α, in contrast to the mild increase in TNF-α production when cells were pretreated with NEM-AQ. Thus, the *in vitro* digestion potentiated the anti-inflammatory action of NEM, so that much lower doses of NEM-IVD were seen to produce similar effects as 25-fold higher doses of NEM-AQ. This is relevant for suggesting anti-inflammatory mechanisms *in vivo* after consumption of NEM and subsequent digestion in the stomach.

The dose–responses seen in the different assays were in several cases nonlinear. This may be attributed to several confounding factors associated with the highest dose, suggesting that the biological effects observed at lower doses should receive the most attention. It may be argued that the highest dose we used (5 g/L) exceeds a likely physiologically relevant dose. However, it may also be argued that this dose may be reached locally along the intestinal mucosa after consumption. We suggest that the highest dose (5 g/L) is quite high and that the biological responses seen at the two lower doses may be more relevant for predicting *in vivo* outcomes. There is also the possibility that calcium may have been an issue at the highest dose. NEM contains some calcium from unseparated eggshell, so for the most part this will be insoluble calcium carbonate. At the 5 g/L dose of NEM, the amount of calcium present may still be sufficient to interfere with cellular signaling. Further dilution of NEM may dilute calcium to insignificant levels. As it is therefore unlikely that calcium contributed to the different responses seen at the lowest dose, it cannot be completely ruled out as a potential mechanism of disturbing or abrogating cellular signaling at the highest dose used.

In the case of the TNF-α cytokine testing, the most interesting difference between the effects of NEM-AQ and NEM-IVD was the reduction in TNF-α production in the

presence of PWM that occurred with all three concentrations of NEM-IVD. These reductions in TNF-α production were strongest with the lowest doses of NEM-IVD, and this effect was opposite to that seen for NEM-AQ. Although the *in vitro* digestion procedure introduced compounds that were not completely removed by the size exclusion centrifugation step and that possessed bioactivity, the digestion process nevertheless increased the ability of NEM-AQ to reduce TNF-α production in 4-day PBMC cultures in the presence of PWM. The effect of NEM-IVD on TNF-α production in the presence of PWM was also different from the effect resulting from treatment of PBMC cultures with PBS-IVD and points to activities unique to the NEM-IVD product.

In particular, the result of NEM-AQ and NEM-IVD reducing TNF-α production is of interest in terms of identifying mechanisms of action pertaining to arthritis conditions because this cytokine is known to attract cell infiltration into arthritic joints and contribute to the inflammation within the joint.

Comparison of the effects of NEM-AQ and NEM-IVD on cytokine production by PBMC cultures revealed some differences that could not be entirely attributed to activities derived from the *in vitro* digestion process itself (such as enzyme breakdown products or residual bile salts that were not removed by the size exclusion centrifugation step). This unique effect of NEM-IVD with respect to TNF-α clearly warrants efforts to further investigate the effects of *in vitro* digestion on NEM. This is of particular importance as several biological TNF-α–inhibiting drugs have proven quite effective in treating arthritis but have been shown to have infrequent but often severe side effects.[24] A treatment, such as NEM, that has immunomodulatory properties that are likely more diffuse could potentially avoid the unfortunate side effects of the currently available biological drugs.

ACKNOWLEDGMENTS

This study was performed at NIS Labs, an independent research lab specializing in natural products research, and was sponsored by ESM Technologies, LLC.

AUTHOR DISCLOSURE STATEMENT

K.F.B. and G.S.J. are employed by NIS Labs, an independent contract research laboratory. K.J.R. is employed by ESM Technologies, LLC in the function of Director of Scientific and Regulatory Affairs. The authors have no other financial interest in the subject matter.

REFERENCES

1. Gonzalez EA: The role of cytokines in skeletal remodeling: possible consequences for renal osteodystrophy. *Nephrol Dial Transplant* 2000;15:945–950.
2. Komano Y, Nanki T, Hayashida K, Taniguchi K, Miyasaka N: Identification of a human peripheral blood monocyte subset that differentiates into osteoclasts. *Arthritis Res Ther* 2006; 8:R152.
3. Tsutsumi H, Tanaka T, Ohashi N, Masuno H, Tamamura H, Hiramatsu K, Araki T, Ueda S, Oishi S, Fujii N: Therapeutic potential of the chemokine receptor CXCR4 antagonists as multifunctional agents. *Biopolymers* 2007;88:279–289.
4. Santiago B, Baleux F, Palao G, Gutierrez-Canas I, Ramirez JC, Arenzana-Seisdedos F, Pablos JL: CXCL12 [SDF-1] is displayed by rheumatoid endothelial cells through its basic amino-terminal motif on heparan sulfate proteoglycans. *Arthritis Res Ther* 2006;8:R43.
5. Ruff KJ, Devore DP, Leu MD, Robinson MA: Eggshell membrane: a possible new natural therapeutic for joint and connective tissue disorders. Results from two open-label human clinical studies. *Clin Interv Aging* 2009;4:235–240.
6. Ruff KJ, Winkler A, Jackson RW, DeVore DP, Ritz BW: Eggshell membrane in the treatment of pain and stiffness from osteoarthritis of the knee: a randomized, multicenter, double-blind, placebo-controlled clinical study. *Clin Rheumatol* 2009;28:907–914.
7. Wong M, Hendrix MJC, von der Mark K, Little C, Stern R: Collagen in the egg shell membranes of the hen. *Dev Biol* 1984;104:28–36.
8. Baker JR, Balch DA: A study of the organic material of hen's-egg shell. *Biochem J* 1962;82:352–361.
9. Long FD, Adams RG, DeVore DP, inventors; New Life Resources, LLC, assignee: Preparation of hyaluronic acid from eggshell membrane. U.S. Patent 6,946,551. September 20, 2005.
10. Picard J, Paul-Gardais A, Vedel M: Sulfated glycoproteins from egg shell membranes and hen oviduct. Isolation and characterization of sulfated glycopeptides. *Biochim Biophys Acta* 1973;320: 427–441.
11. Yun S, Habicht J-P, Miller DD, Glahn RP: An *in vitro* digestion/Caco-2 cell culture system accurately predicts the effects of ascorbic acid and polyphenolic compounds on iron bioavailability in humans. *J Nutr* 2004;134:2717–2721.
12. Boyer J, Brown D, Liu RH: *In vitro* digestion and lactase treatment influence uptake of quercitin and quercetin glucoside by the Caco-2 cell monolayer. *Nutr J* 2005;4:1–15.
13. Toor RK, Savage GP, Lister CE: Release of antioxidant components from tomatoes determined by an *in vitro* digestion method. *Int J Food Sci Nutr* 2009;60:119–129.
14. Jensen GS, Benson KF, Carter SG, Endres JR: GanedenBC30 cell wall and metabolites: anti-inflammatory and immune modulation effects in vitro. *BMC Immunol* 2010;11:15.
15. Sakkas L, Platsoucas C: The role of T cells in the pathogenesis of osteoarthritis. *Arthritis Rheum* 2007;56:409–424.
16. Attur M, Belitskaya-Lévy I, Oh C, Krasnokutsky S, Greenberg J, Samuels J, Smiles S, Lee S, Patel J, Al-Mussawir H, McDaniel G, Kraus VB, Abramson SB: Increased interleukin-1β gene expression in peripheral blood leukocytes is associated with increased pain and predicts risk for progression of symptomatic knee osteoarthritis. *Arthritis Rheum* 2011;63:1908–1917.
17. Börjeson J, Reisfeld R, Chessin LN, Welsh PD, Douglas SD: Studies on human peripheral blood lymphocytes *in vitro*. I. Biological and physicochemical properties of the pokeweed mitogen. *J Exp Med* 1966;124:859–872.
18. Chessin LN, Börjeson J, Welsh PD, Douglas SD, Cooper HL: Studies on human peripheral blood lymphocytes *in vitro*. II. Morphological and biochemical studies on the transformation of lymphocytes by pokeweed mitogen. *J Exp Med* 1966;124:873–884.

19. de Vries E, Lafeber GJ, van der Weij JP, van Buijsen AC, Leijh PC, Cats A: Pokeweed-mitogen induced lymphocyte proliferation: the effect of stimulation on mononuclear phagocytic cells. *Immunology* 1980;40:177–182.
20. Weksler ME, Kuntz MM: Synergy between human T and B lymphocytes in their response to phytohaemagglutinin and pokeweed mitogen. *Immunology* 1976;31:273–281.
21. Hammarström L, Bird AG, Britton S, Smith CI: Pokeweed mitogen induced differentiation of human B cells: evaluation by a protein A haemolytic plaque assay. *Immunology* 1979;38:181–189.
22. Jensen GS, Poppema S, Mant MJ, Pilarski LM: Transition in CD45 isoform expression during differentiation of normal and abnormal B cells. *Int Immunol* 1989;1:229–236.
23. Greaves M, Janossy G, Doenhoff M: Selective triggering of human T and B lymphocytes *in vitro* by polyclonal mitogens. *J Exp Med* 1974;140:1–18.
24. Hochberg MC, Lebwohl MG, Plevy SE, Hobbs KF, Yocum DE: The benefit/risk profile of TNF-blocking agents: findings of a consensus panel. *Semin Arthritis Rheum* 2005;34: 819–836.

This article has been cited by:

1. Jensen Gitte S., Lenninger Miki R., Beaman Joni L., Taylor Robert, Benson Kathleen F.. 2015. Support of Joint Function, Range of Motion, and Physical Activity Levels by Consumption of a Water-Soluble Egg Membrane Hydrolyzate. *Journal of Medicinal Food* **18**:9, 1042-1048. [Abstract] [Full Text HTML] [Full Text PDF] [Full Text PDF with Links]
2. Damian Crowley, Yvonne O'Callaghan, Aoife McCarthy, Alan Connolly, Charles O. Piggott, Richard J. FitzGerald, Nora M. O'Brien. 2015. Immunomodulatory potential of a brewers' spent grain protein hydrolysate incorporated into low-fat milk following in vitro gastrointestinal digestion. *International Journal of Food Sciences and Nutrition* **66**, 672-676. [CrossRef]
3. Yaning Shi, Prithy Rupa, Bo Jiang, Yoshinori Mine. 2014. Hydrolysate from Eggshell Membrane Ameliorates Intestinal Inflammation in Mice. *International Journal of Molecular Sciences* **15**, 22728-22742. [CrossRef]
4. Matej Baláž. 2014. Eggshell membrane biomaterial as a platform for applications in materials science. *Acta Biomaterialia* **10**, 3827-3843. [CrossRef]
5. Kevin J. Ruff, Dale P. DeVore. 2014. Reduction of pro-inflammatory cytokines in rats following 7-day oral supplementation with a proprietary eggshell membrane-derived product. *Modern Research in Inflammation* **03**, 19-25. [CrossRef]

Cell Tissue Res (2011) 345:177–190
DOI 10.1007/s00441-011-1172-z

REGULAR ARTICLE

Hydrolyzed eggshell membrane immobilized on phosphorylcholine polymer supplies extracellular matrix environment for human dermal fibroblasts

Eri Ohto-Fujita · Tomohiro Konno · Miho Shimizu · Kazuhiko Ishihara · Toshihiro Sugitate · Jun Miyake · Kotaro Yoshimura · Kaori Taniwaki · Takashi Sakurai · Yukio Hasebe · Yoriko Atomi

Received: 17 October 2010 / Accepted: 5 April 2011 / Published online: 20 May 2011

Abstract We have found that a water-soluble alkaline-digested form of eggshell membrane (ASESM) can provide an extracellular matrix (ECM) environment for human dermal fibroblast cells (HDF) in vitro. Avian eggshell membrane (ESM) has a fibrous-meshwork structure and has long been utilized as a Chinese medicine for recovery from burn injuries and wounds in Asian countries. Therefore, ESM is expected to provide an excellent natural material for biomedical use. However, such applications have been hampered by the insolubility of ESM proteins. We have used a recently developed artificial cell membrane biointerface, 2-methacryloyloxyethyl phosphorylcholine polymer (PMBN) to immobilize ASESM proteins. The surface shows a fibrous structure under the atomic force microscope, and adhesion of HDF to ASESM is ASESM-dose-dependent. Quantitative mRNA analysis has revealed that the expression of type III collagen, matrix metalloproteinase-2, and decorin mRNAs is more than two-fold higher when HDF come into contact with a lower

Eri Ohto-Fujita and Yoriko Atomi contributed equally to this work.

E. Ohto-Fujita · M. Shimizu
Graduate School of Information Science and Technology,
The University of Tokyo,
7-3-1, Hongo, Bunkyo-ku,
Tokyo 113-8656, Japan

T. Konno · K. Ishihara · T. Sugitate · J. Miyake
Department of Bioengineering, School of Engineering,
The University of Tokyo,
7-3-1, Hongo, Bunkyo-ku,
Tokyo 113-8656, Japan

T. Konno · K. Ishihara
Center for NanoBio Integration, The University of Tokyo,
7-3-1, Hongo, Bunkyo-ku,
Tokyo 113-8656, Japan

K. Ishihara
Department of Materials Engineering, School of Engineering,
The University of Tokyo,
7-3-1, Hongo, Bunkyo-ku,
Tokyo 113-8656, Japan

K. Yoshimura
Department of Plastic Surgery, Graduate School of Medicine,
The University of Tokyo,
7-3-1, Hongo, Bunkyo-ku,
Tokyo 113-8656, Japan

J. Miyake
Department of Mechanical Science and Bioengineering,
Graduate School of Engineering Science, University of Osaka,
1-3, Machikaneyama, Toyonaka,
Osaka 560-8531, Japan

K. Taniwaki · Y. Hasebe
Almado incorporation,
2-46-2 Honcho, Nakano-ku,
Tokyo 164-0012, Japan

T. Sakurai
Department of Life Science, Graduate School of Arts & Science,
The University of Tokyo,
Komaba 3-8-1, Meguro-ku,
Tokyo 153-8902, Japan

Y. Atomi (✉)
Radioisotope Center, The University of Tokyo,
2-11-16, Yayoi, Bunkyo-ku,
Tokyo 113-0032, Japan
e-mail: atomi@bio.c.u-tokyo.ac.jp

dose ASESM proteins immobilized on PMBN surface. A particle-exclusion assay with fixed erythrocytes has visualized secreted water-binding molecules around the cells. Thus, HDF seems to possess an ECM environment on the newly designed PMBN-ASESM surface, and future applications of the ASESM-PMBN system for biomedical use should be of great interest.

Keywords Extracellular matrix · Eggshell membrane · Phospholipid polymer · Dermal fibroblasts · Type III collagen · Human

Abbreviations

ESM	Eggshell membrane
ECM	Extracellular matrix
ASESM	Alkaline-digested form of ESM
HDF	Human dermal fibroblasts
AFM	Atomic force microscopy
MPC	2-Methacryloyloxyethyl phosphorylcholine
MEONP	*p*-Nitrophenyloxycarbonyl poly(oxyethylene) methacrylate
BMA	*n*-Butyl methacrylate
PMBN	Poly(MPC-*co*-BMA-*co*-MEONP)
TC	Tissue culture
GAPDH	Glyceraldehyde-3-phosphate dehydrogenase
MMP	Matrix metalloproteinase
HAS2	Hyaluronan synthetase 2
GAG	Glycosaminoglycan
PBS	Phosphate-buffered saline
FGF-2	Fibroblast growth factor-2
TGF-β	Transforming growth factor-β

Introduction

Extracellular matrices (ECM) not only serve a structural function providing support and strength to cells within tissues, but also determine critical cellular functions through cell-matrix interactions (Bruckner 2010). The unique architecture and characteristics of tissues and organs are determined by the ECM and the cells that produce it. ECM proteins can be classified into four general categories: collagens, structural glycoproteins, proteoglycans, and elastins (Tsang et al. 2010). In the dermis, heterotypic collagen fibrils containing mainly collagens I, III, and V are the major structural components responsible for its characteristic strength and resilience. Cell adhesion to ECM proteins through physical association with integrins is associated with intracellular signaling events and is critical for successful tissue regeneration (Grzesiak et al. 1997). Mechanical force increases the gene expression for collagen I and III in cycle-stretched cells obtained from ligament, such as anterior cruciate ligament cells (Kim et al. 2002) and bone-marrow-derived mesenchymal stroma cells (Zhang et al. 2008). ECM also plays important functional roles in interacting with numerous growth factors and signaling molecules to regulate cellular events such as cell adhesion, proliferation, migration, survival, and differentiation. Collagens are triple helical proteins that confer compressive and tensile strength to animal tissues and serve as anchors for cell adhesion through surface receptors.

Eggshell membrane (ESM), a functional equivalent of ECM in avian egg during development, is a double-layered insoluble sheet located between the eggshell and egg white and acts as a scaffold for biomineralization to fabricate the egg shell (Rose and Hincke 2009). The membrane is formed in the isthmus of the oviduct of the hen before shell mineralization and egg laying (Rose and Hincke 2009). ESM has a fibrous network mainly comprised of type I, V, and X collagens, glucosamine, desmosin, and hyaluronic acid (Ha et al. 2007; Osuoji 1971; Wong et al. 1984) and is cross-linked by lysyl oxidase (Harris et al. 1980). ESM also has antibacterial and antimicrobial activities to resist bacterial invasion (Ahlborn and Sheldon 2005) and thereby protect the developing embryo (Burley and Vadehra 1989). Recently, ESM-containing cosmetics and supplements have come onto the market worldwide, based on the evidence from traditional folk medicine in Asian countries. For more than four hundred years, ESM has been used to cure injuries, and the prescription appears in the pharmacopoeia of Chinese medicine, Bencao Gangmu. In Japan, Sumo wrestlers use ESM as a natural medicine for injuries. All this evidence suggests that ESM promotes wound healing. However, no molecular mechanism has been studied yet. Wound healing is a four-step sequential event including hemostasis, inflammation, proliferation, and remodeling (Diegelmann and Evans 2004). During these processes, tissue disruption has to be repaired and filled by ECM molecules (e.g., mainly collagen) deposited by dermal fibroblast cells.

In this study, we have aimed to construct a model system for the evaluation of ESM function on dermal fibroblast adhesion and the production of ECM components in vitro. Recently, the construction and modification of biomimetic surfaces has been targeted to support tissue-specific cell functions including adhesion, growth, differentiation, motility, and the expression of tissue-specific genes (von der Mark et al. 2010). We have used a novel artificial cell membrane biointerface, viz., a poly(2-methacryloyloxyethyl phosphorylcholine [MPC]-*co*-*n*-butyl methacrylate [BMA]-*co*-*p*-nitrophenyloxycarbonyl poly(oxyethylene) methacrylate [MEONP]) (PMBN; Konno et al. 2004) to immobilize alkaline water-miscible organic-solvent-hydrolyzed soluble eggshell membrane (ASESM) molecules. Phosphorylcholine group in the PMBN provides excellent biointerfaces, and these interfaces facilitate the suppression of nonspecific protein adsorption and stabilization of immobilized biomolecules (Watanabe and Ishihara 2007). BMA unit is hydropho-

bic polymer backbone, which can cover on the surface of substrates such as polystyrene tissue culture dish. MEONP unit contains active ester groups for the conjugation of the amino group of biomolecules via oxyethylene chain (Konno et al. 2004). Although accelerated cell growth of fibroblasts has been observed on an acid oxidized-pepsin digested ESM crosslinked to pepsin-solubilized collagen coat (Ino et al. 2006), our system has a unique advantage for the analysis of the molecular mechanism of ESM-fibroblast interaction. Since cells do not adhere at all to the conventional MPC polymer itself, unlike to collagen-coated dishes or polystyrene cell culture dishes, any specific and direct effects of ASESM molecules on fibroblast adhesion can be tested.

Materials and methods

ASESM molecules

ASESM, which is hydrolyzed ESM digested in alkaline water-miscible organic solvent (EM PROTEIN-P), was purchased from Q.P. (Tokyo, Japan).

Microscopic ESM observation

Avian ESM was removed from eggshell, washed with water, and placed on the slide glass. The surface of the membrane was observed by means of a TCS-SP5 confocal microscope (Leica microsystems, Wetzlar, Germany) with a 488 argon laser.

Atomic force microscopy

The pyramidal-shaped silicon probe (OMCL-TR400PSA-1, 0.08 N/m) for atomic force microscopy (AFM) was purchased from Olympus (Tokyo, Japan). An MPC polymer such as PMBN was coated onto mica and dried. The mica was placed in a 12-well plate, and then 1 mg/ml or 30 mg/ml ASESM was conjugated to it. AFM images of ASESM-conjugated PMBN and non-conjugated control PMBN on mica were taken by using a Nanowizard II (JPK Instruments, Berlin, Germany) in intermittent contact mode in liquid.

Molecular weight estimation of ASESM proteins by size-exclusion chromatography

The molecular weight of ASESM proteins was estimated by size-exclusion chromatography on a Superose 6 HR 10/30 1.0 cm×30 cm size-exclusion column (GE Healthcare, USA) by using high performance liquid chromatography (Waters 640) with the following mobile phase: phosphate-buffered saline (PBS: 137 mM NaCl, 8.1 mM $Na_2HPO_4 \cdot 12 H_2O$, 2.68 mM KCl, 1.47 mM KH_2PO_4), at a flow rate of 0.3 ml/min. Thyroglobulin (670 kDa), γ-globulin (158 kDa), ovalbumin (44 kDa), myoglobin (17 kDa), and Vitamin B_{12} (1.35 kDa) in a gel-filtration standard (BioRad) were used to calibrate the column.

Cell culture

Human dermal fibroblasts (HDF) derived from infant skin were isolated as described previously (Aiba-Kojima et al. 2007). HDF were cultured with Dulbecco's modified Eagle's medium (Wako Pure Chemical Industries) containing 10% fetal bovine serum (Sigma-Aldrich), 0.1 mg/ml Kanamycin sulfate (Meiji Seika Kaisha), and a penicillin-streptomycin-neomycin (PSN) antibiotic mixture (1×; Gibco). HDF of passage number 8 were used in this study.

Synthesis of the PMBN

Methods for preparing PMBN were as previously described by Konno et al. (2004).

Dish coating

Polystyrene tissue culture (TC) dishes (35 mm; Falcon 353001, BD Biosciences) were coated with 0.2% PMBN, dried in an ethanol atmosphere, coated with 1 ml of various concentrations of ASESM (0, 1, 5, 10, 30, 100 mg/ml Milli-Q ultrapure water; Millipore) at 4°C for 24 h, and then washed with PBS several times. Unreacted active ester units were blocked with 100 mg/ml glycine at room temperature for 2 h. Before cells were inoculated, the dishes were washed again with PBS. For control non-conjugated PMBN experiments, the active ester units in the PMBN coated surface were inactivated with glycine. PMBN dishes blocked with glycine were prepared. As another control experiment, collagen-coated dishes were prepared as follows: a TC dish was treated with 0.3 mg/ml collagen (from calf skin; Sigma, C9791) in hydrochloric acid solution (pH 3.0) for 5 min, air-dried, and rinsed with PBS. Cells were observed with an inverted microscope (Zeiss), and images were captured by a charge-coupled device camera (Orca, Hamamatsu, Japan). The brightness and contrast of images were adjusted by Adobe Photoshop Elements v. 6.0.

Quntitative gene expression analysis of HDF with or without ASESM

Total RNA from HDF cultured for 24 h was extracted by means of the High Pure RNA Isolation Kit (Roche Applied Science, Mannheim, Germany) according to the manufacturer's protocol. First-strand cDNA was synthesized by using PrimeScript RT reagent kit (Perfect Real Time; Takara Bio). The primer and probe oligonucleotides for targeting human genes were designed by utilizing the Universal ProbeLibrary Assay Design Center (Roche Applied Science). All oligonu-

cleotides were obtained from Nihon gene research laboratories (Sendai, Japan). Amplification of the housekeeping gene glyceraldehyde-3-phosphate dehydrogenase (GAPDH) mRNA, which served as a normalization standard, was carried out with GAPDH primers 5′-AGCCACATCGCTCAGACAC-3′ (sense) and 5′-GCCCAATACGACCAAATCC-3′ (anti-sense). The gene-specific primers for COL3A1 were 5′-GGACCTCCTGGTGCTATAGGT-3′ (sense) and 5′-CGGGTCTACCTGATTCTCCAT-3′ (anti-sense), for COL1A1 were 5′-GGGATTCCCTGGACCTAAAG-3′ (sense) and 5′-GGAACACCTCGCTCTCCA-3′ (anti-sense), for matrix metalloproteinase 2 (MMP2) were 5′-GAGG TAATCTTAGGTGCTTACCTAGC-3′ (sense) and 5′-CTTCAGCACAAACAGGTTGC-3′ (anti-sense), for metalloproteinase 3 (MMP3) were 5′-CAAAACATATTTCTTTG TAGAGGACAA-3′ (sense) and 5′-TTCAGCTATT TGCTTGGGAAA-3′ (anti-sense), for hyaluronan synthetase 2 (HAS2) were 5′-CTCCGGGACCACACAGAC-3′ (sense) and 5′-TCAGGATACATAGAAACCTCTCACA-3′ (anti-sense), for elastin were 5′-CACTGGGGTATCCCATCAAG-3′ (sense) and 5′-GTGGTGTAGGGCAGTCCATAG-3′ (anti-sense), for decorin were 5′-GGAGACTTTAAGAACCT GAAGAACC-3′ (sense) and 5′-CGTTCCAACTTCAC CAAAGG-3′ (anti-sense), and for biglycan were 5′-CAGCCCGCCAACTAGTCA-3′ (sense) and 5′-GGCCAG CAGAGACACGAG-3′ (anti-sense).

For the quantitative real-time polymerase chain reaction (PCR) analysis, an aliquot of 1 μl cDNA (25 ng total RNA equivalent) was added to 19 μl of the reaction mixture containing 1× Taqman Universal PCR Master Mix (Applied Biosystems), 900 nM forward/reverse primer, and 250 nM Universal ProbeLibrary probe (Roche). Standard GAPDH-based real-time PCR was performed by using the Applied Biosystems 7500 Fast Real-Time PCR System, and the following PCR cycle was employed: initial denaturation at 95°C for 20 s and then 40 cycles of amplification (denaturing at 95°C for 3 s and annealing and polymerization at 60°C for 30 s).

To analyze the ASESM dose-dependency of the ECM-related gene expression pattern, trendlines were calculated and added by Microsoft Office Excel 2007. The best line type was chosen from five different trends (linear approximation, power approximation, exponential approximation, log approximation, polynomial approximation), so that its R-squared value was at or near 1.

Immunofluorescence of HDF

Cells were cultured on cover glasses (22 mm×22 mm, 0.12-0.17 mm thick, Matsunami Glass) in a 35-mm TC dish for 24 h. Cells were briefly washed with PBS and fixed at room temperature in Fix1 (4% paraformaldehyde, 2 mM $MgCl_2$, and 2 mM EGTA in PBS) for 10 min. The cells were then washed several times with PBS and permeabilized with Fix2 (0.03% Triton X-100 in Fix1) for 10 min at room temperature. Fixed cells were washed several times with PBS and blocked in PBS containing 1% (w/v) bovine serum albumin and 0.02% sodium azide. Cells were incubated with goat polyclonal anti-procollagen type I antibody (SC-8783, Santa Cruz) overnight at 4°C, washed with PBS, followed by incubation with DyLight-488-conjugated anti-goat IgG (H&L) antibody (Rockland Immunochemicals for Research) for 1 h at room temperature. Images were taken by using a TCS-SP5 confocal microscope (Leica microsystems, Wetzlar, Germany). The brightness and contrast of images were adjusted by Adobe Photoshop Elements v. 6.0.

Particle-exclusion assay

To visualize the highly hydrated pericellular matrix around adhered HDF, the fluorescent version of the particle-exclusion assay using fixed sheep erythrocytes was performed. HDF (1.5×10^4 cells/well) was inoculated into 24-well EZVIEW Glass Bottom Culture Plates LB (ASAHI Glass). After 24 h, WGA (wheat germ agglutinin) Alexa Fluor 488 conjugate (W11261, Molecular probes) at 5 mg/ml in PBS was added to the culture plate for plasma membrane staining, incubated for 10 min at 37°C, and then washed off with PBS. Fixed sheep erythrocytes (5×10^7; Inter-Cell Technologies) were reconstituted and pre-stained with Alexa-488-WGA in PBS, and then excess fluorescent reagent was washed out. Membrane-stained erythrocytes were added to the culture plate, and the cells were visualized with a LSM510 meta confocal microscope (Zeiss).

To estimate the size of the pericellular coat, the distance between the cell outline and the erythrocyte particle was measured (Simpson et al. 2009) by the LSM image browser (Zeiss).

Results

Physical property of ASESM conjugated to PMBN

The fibril meshwork of the natural avian ESM was observed by confocal microscopy (Fig. 1a). ESM is not a water-soluble material, because it is composed of highly cross-linked ECM molecules. Although commercially available ASESM powder is easy to dissolve to at least 40% (w/v) in ultra-pure water at room temperature, undigested and/or re-assembled fibril structure is postulated to remain in the ASESM because of its highly complex fibril architecture (Fig. 1a). The relative molecular weight of ASESM was analyzed by gel filtration, and its main mass was found to be about 12–14 kDa (Fig. 1b). Newly designed ASESM-PMBN was prepared by covalent bond formation between ASESM

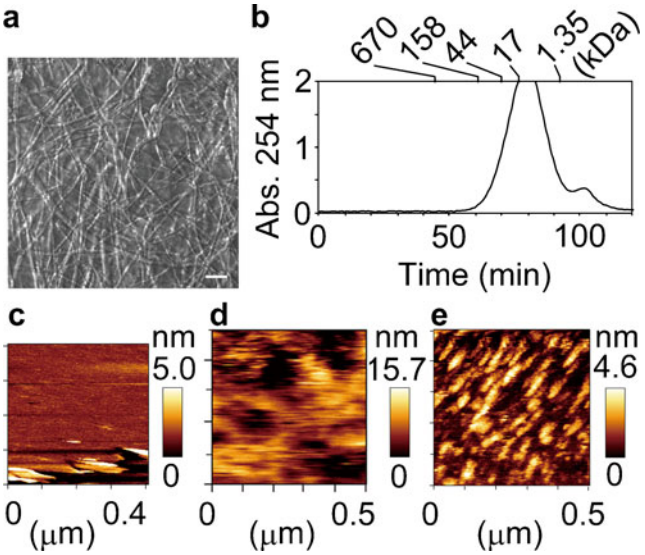

Fig. 1 **a** Microscopical image of eggshell membrane (ESM). *Bar* 100 μm. **b** Distribution of molecular weight of alkaline water-miscible organic-solvent-hydrolyzed soluble eggshell membrane (ASESM) molecules as estimated by size-exclusion chromatography. Five molecular weight protein standards are indicated *above* the chart corresponding to the respective elution time. **c–e** Fibril structures forming when 30 mg/ml ASESM is conjugated to PMBN [poly(2-methacryloyloxyethyl phosphorylcholine-*co*-*n*-butyl methacrylate-*co*-*p*-nitrophenyloxycarbonyl poly(oxyethylene) methacrylate)]. AFM images when 0 mg/ml (**c**), 1 mg/ml (**d**), or 30 mg/ml (**e**) ASESM is conjugated to PMBN on mica. Full color range corresponds to a vertical scale of 4.6–15.7 nm

proteins and PMBN, which has active ester groups (Konno et al. 2004). AFM analysis of ASESM-PMBN applied to mica showed a distinct fiber-like structure when 30 mg/ml ASESM was used for PMBN conjugation (Fig. 1e) but at not the lower concentration of ASESM (1 mg/ml; Fig. 1d). As a control, PMBN alone did not give any detectable structure (Fig. 1c). The typical 67-nm banding pattern of collagen fibrils was not observed in ASESM-PMBN, which is consistent with the result for ESM reported by Wong et al. (1984). ESM is a double-layered fibrous membrane consisting of cross-linked ECM proteins and is formed by lysyl oxidase secreted by the cells inside the hen oviduct during egg formation (Harris et al. 1980). A detailed structural analysis of ASESM fibrils on PMBN will be interesting, because this newly prepared biointerface provides a natural nano-scale fibrous scaffold for HDF as described below.

Adhesion of HDF to ASESM conjugated to PMBN

HDF adhesion to ASESM was initially tested in a plane TC dish. Either with or without ASESM pre-coating, cells adhered to the dish with no detectable difference (data not shown). To obtain a dish surface to which HDF adhered only when ASESM was present, a cytiocompatible MPC polymer bearing active ester units, PMBN (Konno et al. 2004) was used, which can immobilize biomolecules (e.g., proteins, polysaccharides, and DNA) via covalent bond formation between the amino groups of target biomolecules and active ester units in the polymer under mild conditions. First, PMBN was coated onto a TC dish, and then various concentrations of ASESM (0, 1, 5, 10, 30, 100 mg/ml) were applied for conjugation (Fig. 2a-f). Non-reacted active ester groups in the PMBN were blocked by incubation with glycine, and then the dishes were washed with PBS before 8×10^4 HDF were seeded into them. After 24 h, cells were observed under the inverted microscope. We found that HDF had adhered to the ASESM-PMBN dishes (Fig. 2b-f) specifically, as compared with control glycine-conjugated PMBN dishes without ASESM (Fig. 2a). When more than 30 mg/ml ASESM was used for conjugation with the PMBN, the cell culture became semiconfluent (Fig. 2e, f), as in the dishes coated with type I collagen (Fig. 2g) and in untreated TC dishes (Fig. 2h). Interestingly, the mode of cell adhesion was ASESM dose-dependent when used with PMBN conjugation (Fig. 2b-f), but not with respect to the number of the cells inoculated. Notably, cells were relatively round and seemed not to be fully attached to the matrix formed by the lower does of ASESM (1 mg, 5 mg/ml ASESM-PMBN in Fig. 2b, c, i). However, on the ASESM scaffold in which higher doses of ASESM were conjugated to the PMBN, the cells were extended and flat (Fig. 2f, k, n, p), similar to the cells on control TC/collagen-coated dishes (Fig. 2h, l, m, o), and fully adhered to the matrix regardless of the cell density on the ASESM surface (adjusted by number of cells seeded). The morphology of HDF on ASESM at 10 mg/ml (Fig. 2j) showed an intermediate structure between the cells on ASESM at 5 mg/ml (Fig. 2i) and ASESM at 100 mg/ml (Fig. 2k) /control TC dish (Fig. 2l). These different cell adhesion modes, which various doses of ASESM were used for PMBN conjugation, may reflect the surface structure (fibril plus or minus) as observed in AFM analysis (Fig. 1d, e).

ECM-related gene expression of HDF on ASESM conjugated to PMBN

Expression of the major ECM-related genes from HDF attached to different doses of the ASESM-conjugated matrix was examined by a standard quantitative real-time PCR protocol, and the gene expression pattern as a function of ASESM dose was analyzed by a curve fitting method (Fig. 3). The gene expression pattern of type III collagen (Fig. 3a), decorin (Fig. 3g), and MMP2 (also known as gelatinase A, Fig. 3e) at the various doses of ASESM was fitted with a power approximation curve, unlike the other genes: type I collagen (Fig. 3b), elastin (Fig. 3c), MMP3 (Fig. 3d), biglycan (Fig. 3h), and HAS2 (Fig. 3f). Interestingly, at the lower doses of ASESM conjugated to the MPC surface (1 mg/ml ASESM, the leftmost graph in each individual gene

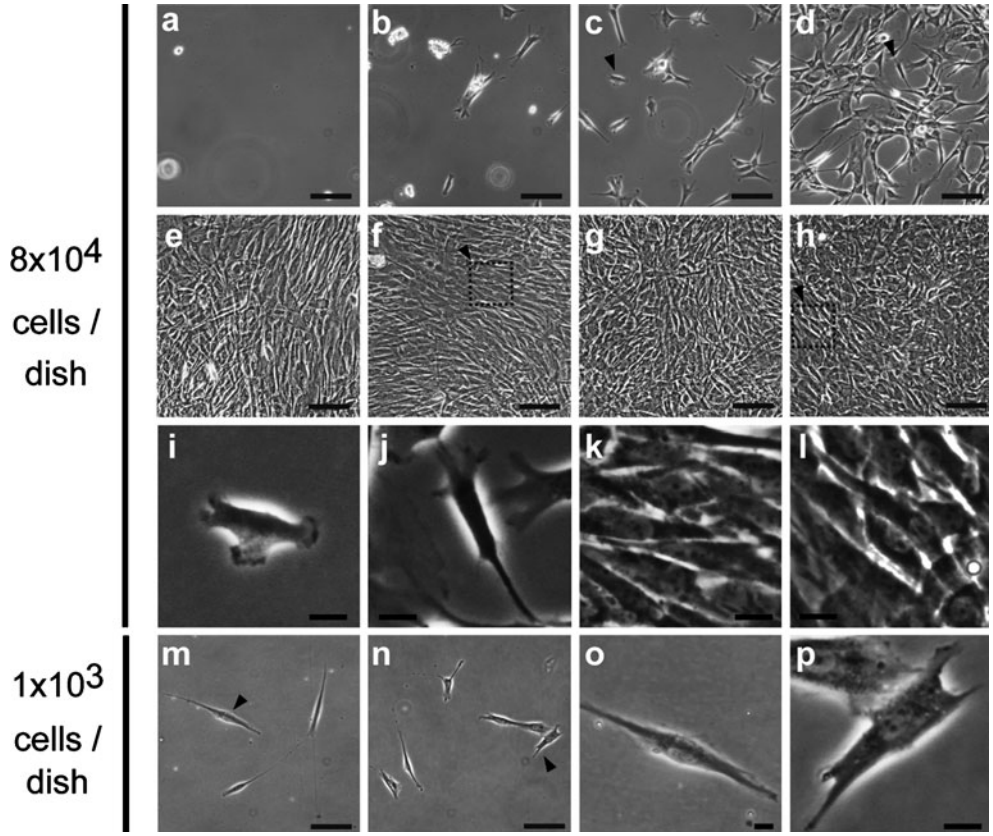

Fig. 2 HDF adheres preferentially to ASESM fibril structure, and the mode of HDF adhesion is controlled by the ASESM dose, which affects the fibril structure on PMBN, but not by the population of the cells. **a**–**h** HDF at 8×10^4 cells/dish were grown on 0 mg/ml (**a**), 1 mg/ml (**b**), 5 mg/ml (**c**), 10 mg/ml (**d**), 30 mg/ml (**e**), or 100 mg/ml (**f**) ASESM conjugated to PMBN as a matrix, on a collagen matrix (**g**), or on a control (directly on tissue culture [TC] dish) surface (**h**). *Bars* 100 μm. **i**, **j** Representative cells in **c**, **d** (*arrowheads*), respectively, at higher magnification. **k**, **l** *Dotted boxes* with *arrowhead* in **f**, **h**, respectively, at higher magnification. *Bars* 20 μm. **m**, **n** HDF at 1×10^3 cells/dish were grown on a control collagen matrix) or on 100 mg/ml ASESM conjugated to PMBN, respectively. *Bars* 100 μm. **o**, **p** Representative cells in **m**, **n** (*arrowheads*), respectively, at higher magnification. *Bars* 20 μm

set in Fig. 3), the mRNA expression level of type III (Fig. 3a) but not type I collagen (Fig. 3b), MMP2 (Fig. 3e), and decorin (one of the proteoglycans that contains one chondroitin/dermatan sulfate GAG side-chain, Fig. 3g) was markedly increased by more than two-fold compared with control TC or collagen-coated dishes (Fig. 3a, e, g, inset). Other ECM-related genes such as type I collagen (Fig. 3b), elastin (Fig. 3c), MMP3/stromelysin-1 (Fig. 3d), and biglycan (Fig. 3h) showed similar mRNA expression levels as the control, with no ASESM dose-dependency. Expression of another ECM constituent, HAS2, which has a high molecular weight with unbranched polysaccharide extruded to the extracellular space, increased about three-fold depending on ASESM dose but was the same level as control (Fig. 3f). From these mRNA expression analyses, type III collagen, MMP2, HAS2, and decorin were found to be direct/indirect-response genes of HDF by ASESM proteins. Further study (e.g,. time-course of gene and protein expression and identification of the related growth factors/cell signaling mechanism) will clarify the ASESM/ESM function toward HDF.

Visualization of ECM proteins and glycosaminoglycan in HDF: type I collagen and pericellular ECM

We also analyzed the ECM-related gene expression at the cellular level with or without ASESM in HDF by antibody detection of type I collagen and by particle-exclusion assay for detecting the highly hydrated ECM at the pericellular space (Fig. 4). HDF were grown on an ASESM surface (Fig. 4c, d), on a surface coated with type I collagen (Fig. 4b), or on glass (Fig. 4a) and fixed. Indirect immunofluorescence detection of procollagen type I was performed. The antibody recognizes the procollagen in the endoplasmic reticulum. The localization pattern was similar between the cells on the type I collagen coat (Fig. 4b) and on higher doses of the ASESM conjugated surface (Fig. 4c, d) consistent with the result as shown in Fig. 2o, p.

ECM-related glycosaminoglycan (GAG), such as decorin and hyaluronan (gene product of HAS2), is responsible for various cellular function including adhesion and wound healing (Laurent and Fraser 1992). GAG is a highly hydrophilic molecule that exists on the cell surface and binds a large amount of water around the cell. Visualization of such a pericellular coat can be achieved by the reported particle-exclusion assays on fixed erythrocytes for hyaluronan detection (Itano et al. 1999; Fig. 4e-h). The distance from the cell surface to the excluded area is similar between low and high doses of ASESM. Although the HAS2 expression was relatively low for HDF on lower dose of ASESM surface (Fig. 3f), HDF appeared to secrete similar amounts of pericellular coat as on other culture surfaces. A relatively clear exclusion pattern was seen for the cells on a lower dose of ASESM surface (Fig. 4f). This might be correlated to the higher decorin mRNA expression (Fig. 3g),

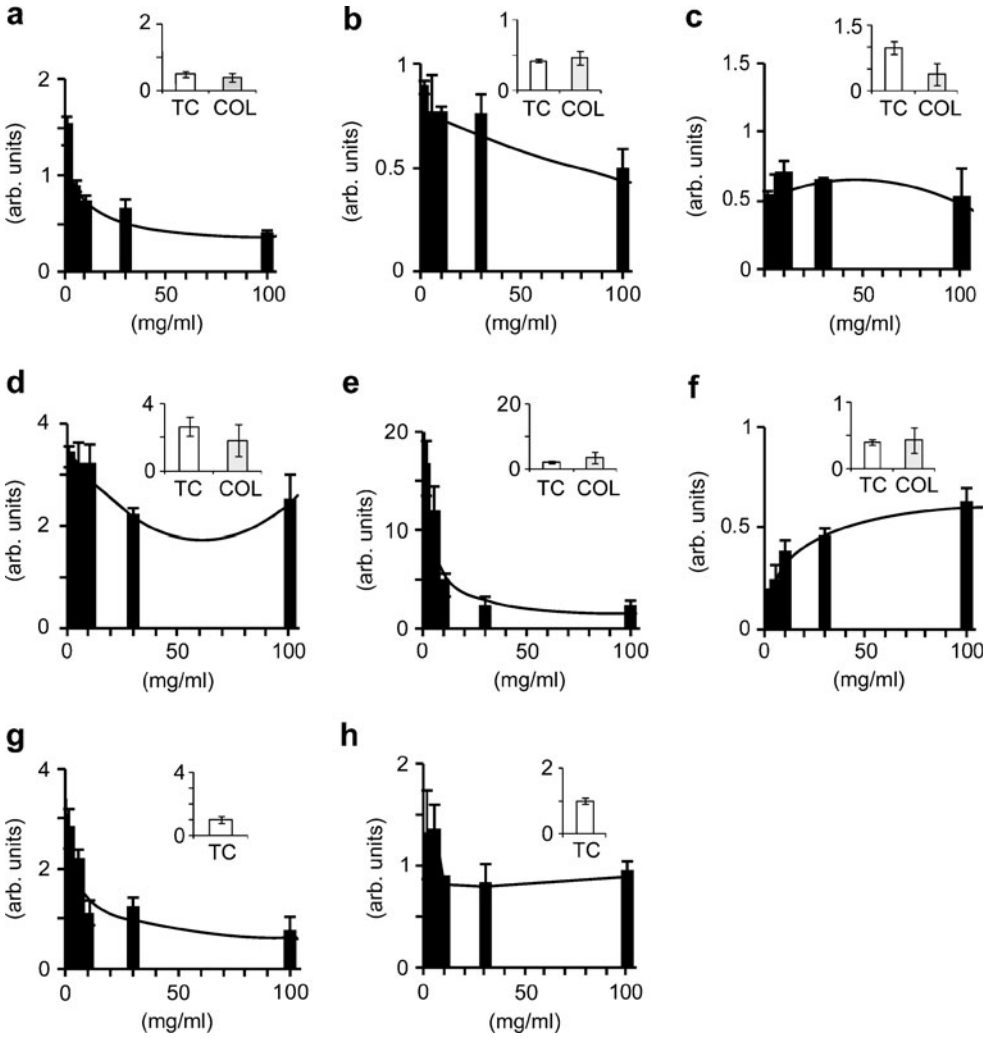

Fig. 3 Relative gene expressions of HDF on various amounts of ASESM (1, 5, 10, 30, 100 mg/ml) conjugated to PMBN as normalized with glyceraldehyde-3-phosphate dehydrogenase: type III collagen (COL3; **a**), COL1 (**b**), elastin (**c**), matrix metalloproteinase (MMP3; **d**), MMP2 (**e**), hyaluronan synthetase 2 (**f**), decorin (**g**), and biglycan (**h**). The assay was carried out on triplicate samples with 500 ng total RNA recovered from each dish. The data are presented as means±SD (*arb. units* arbitrary units). The fitted curves are as described. *Insets* Relative gene expressions in HDF on either dishes coated with type I collagen (*COL*) or untreated tissue culture dishes (*TC*). Horizontal axis in each graph represents various concentrations of ASESM conjugated to PMBN (mg/ml)

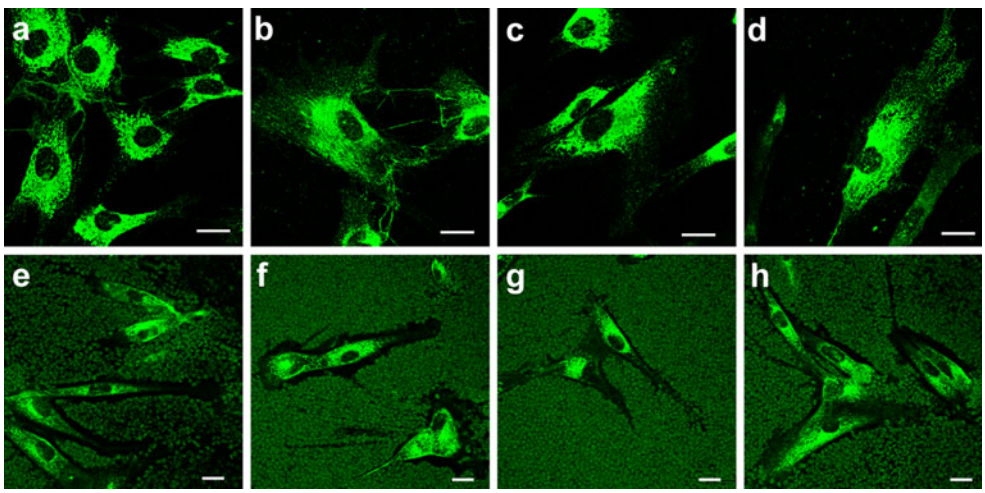

Fig. 4 Visualization of type I collagen protein and particle-exclusion assay on HDF. Cells were grown on glass (**a**), a collagen coat (**b**), 30 mg/ml ASESM-PMBN coat (**c**), or 100 mg/ml ASESM-PMBN coat (**d**). *Bar* 20 μm. Highly hydrated ECM-related glycosaminoglycan coat around HDF grown on glass (**e**), or on 1 mg/ml (**f**), 10 mg/ml (**g**), or 100 mg/ml (**h**) ASESM-PMBN coat. *Bars* 20 μm

and/or the distinct motility of the cells (Evanko et al. 1999) might responsible for this observation as previously described in Fig. 3. The distance from cell surface to excluded area is not different between low and high doses of ASESM. These data show that HDF on the ASESM surface secrete a pericellular coat, including hyaluronan, as on other culture surfaces.

Discussion

We have developed a new in vitro system to study ESM function with respect to HDF adhesion by applying the PMBN. ESM is a readily available natural biomaterial everywhere in the world and can be used in the biomedical, nutritional, and cosmetic fields. The membrane is a highly cross-linked meshwork mainly consisting of ECM molecules such as collagens, proteoglycans, and GAG. A commercially available, alkaline-hydrolyzed version of ESM, ASESM, has been used in this study. Based on AFM analysis, ASESM has been found to adopt a distinct fibril structure compared with the original ESM, either because hydrolysis-tolerating fibers remain and/or hydrolyzed ECM are reassembled de novo on PMBN. An analysis of this assembly process will be interesting from two different viewpoints: (1) in order to understand the HDF adhesion mode and to develop a new biointerface by using ESM and thereby providing different cell adhesion and gene expression properties, and (2) in order to understand an as yet unknown eggshell/shell membrane formation mechanism inside the oviduct of the hen, a mechanism expected to provide hints for designing new biomaterials.

In this study, specific dish surface ASESM conjugated to PMBN was prepared and tested for HDF adhesion. Cells adhere to ASESM on PMBN specifically (Fig. 5b, c) but not to glycine-blocked PMBN (Fig. 5a), and ECM genes are expressed. The most notable finding from our study is that ECM gene expression is significantly altered simply by the cell density and microenvironment of the cells and suggests the following two important points: first, the specific dish surface of ASESM conjugated to PMBN provides a useful in vitro experimental culture system mimicking the actual cell environment inside our living human body; second, the present study provides the first mechanistic insight into the reason that ESM encourages scarless wound healing, as has been known for many years in Asian countries.

Fibroblasts are generally and widely used cultured cells in the field of biological sciences and almost all reported experiments are performed under confluent cell conditions with no thoughts of the in vivo situation. If we look at any of the histological images from tissue sections or the in vivo images of dermis, tendon, and joints in our body, we can readily notice that fibroblasts are dispersed and not "confluent". In spite of the importance of ECM, few studies have investigated tissue origin-dependent cell-ECM interactions or cell-cell interactions in vivo. To visualize such interactions, a histological approach is commonly used, but the dynamic response of the cells to the environments and the modulation of the cytoskeleton and ECM cannot be studied. In the case of recently developed induced pluripotent stem cells (iPS; Takahashi and Yamanaka 2006), robust and intensive studies have been performed world-wide, and a quick shift from basic research to practical applications has been brought about, because such investigations are based on an easily controllable, in vitro cell culture technology. With in vitro systems, cells that survive in various regions of the body (tissue) can be analyzed not only under various nutritional factor conditions, but also with regard to the stiffness of their substrate (Discher et al. 2005). Three-dimensional culture systems are certainly more preferable than two-dimensional systems, because

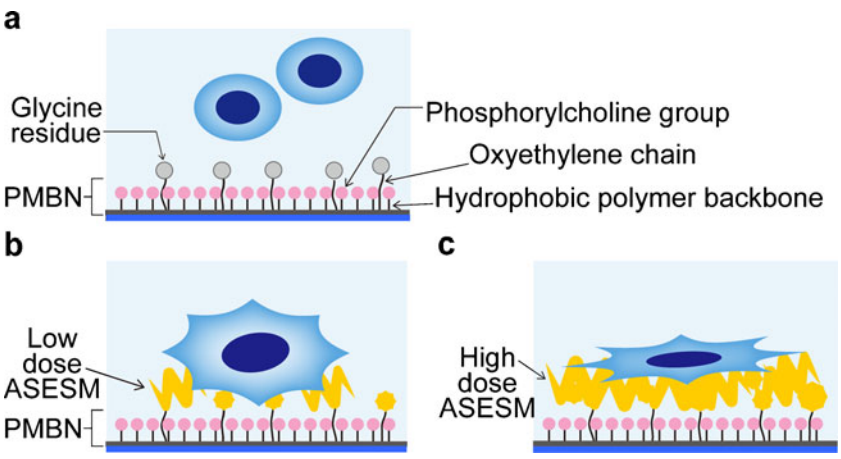

Fig. 5 Characteristic features of the ASESM-PMBN system. **a** Without ASESM, cells do not adhere to PMBN, because unreacted active ester groups were blocked with glycine. **b** Low dose of ASESM conjugated to PMBN provides early wound healing model. **c** High dose of ASESM conjugated to PMBN provides a more stretched and rigid environment

they more closely resemble in vivo conditions, and the mechanical character of ECM and the change of gene expression induced by an environmental cue can be detected (von der Mark et al. 2010). However, complex three-dimensional systems are not always necessary for the direct analysis of the cells responding to a specific biomaterial, as described in this study. Gene expression supplies the ECM environment to HDF, and this may partially explain the biomedical function of ESM for the healing of skin injuries (wound healing). Indeed, Rinn et al. (2008) have demonstrated that dermal fibroblasts are developmentally regulated by particular HOX genes dependent on the different regions in the body. Fibroblasts originating from other skin regions of the body or connective tissues might respond to ASESM differently from those taken from the auricle as used in this study. Our newly developed experimental system might be suitable for investigating site-specific cell response in general. Further studies should clarify the complex biological mechanism regarding the association of HDF and other adhesive cells to ASESM, by adding/subtracting the involved factors in a step-by-step fashion.

We have studied mRNA expression by the quantitative real-time PCR analysis of HDF grown on ASESM. ECM-related genes, which might contribute to maintaining the extracellular environment for healthy dermis, such as those for type III collagen (Vitellaro-Zuccarello et al. 1992), MMP2 (Kahari and Saarialho-Kere 1997), and decorin (Nomura 2006), show a more than two-fold higher expression when cells are grown at a lower dose of ASESM on a surface than when they are cultured on a control dish surface. In the contrast, HAS2 expression is high at a higher dose of ASESM on the surface.

Cutaneous wound healing is a dynamic process that involves the coordinated and sequential deposition of ECM, leading to the formation of a scar. In this study, during the culture of HDF on ASESM for just 24 h, an interesting pattern of gene expression of ECM components including collagen, proteoglycans and hyaluronan and their proteases has been observed, as a function of the applied ASESM quantity. This ASESM dose-dependency seems to be consistent with the temporal expression pattern of ECM molecules during sequential wound healing process. The ECM expression pattern in low-dose ASESM is similar to the early phase, whereas that at a high dose resembles the late phase of wound healing. To analyze the ASESM dose-dependency of ECM-related gene expression patterns, a trendline can be added to the graph by a curve fitting method (Fig. 3). Type III collagen, decorin, and MMP2 are strongly expressed in the early phase of wound healing. In our study, the expression pattern of these three genes have been fitted into a downward power approximation toward the high ASESM dose, whereas other genes have been fitted by the binomial equation, exponential equation, or log approximation. Interestingly, the ASESM dose-dependent increment of HAS2 mRNA fits an upward exponential equation. Although we have not checked the gene expression at a time point other than 24 h, the level of mRNA expression of these wound-healing-related genes at different ASESM concentrations matches the gene expression during the course of sequential events of cutaneous wound healing in vivo; lower ASESM providing an environment similar to the early steps, and higher ASESM for late steps. Based on our AFM analysis (Fig. 1c-e), ASESM seems to adopt a distinct fibril structure depending on the concentration of ASESM applied to PMBN for conjugation, either because the hydrolysis-tolerating fibers remain and/or hydrolyzed ECM are reassembled de novo on PMBN.

Since mutations for both type III (Liu et al. 1997) collagen and decorin (Jarvelainen et al. 2006) are not lethal in the mouse, these genes are not essential for survival but are important for providing a soft environment within tissues and play roles in modulating the ECM environment, being responsible for elastic young skin, for human health, and for body maintenance in aged people. The major function of type III collagen is associated with the fibrogenesis of type I collagen (Liu et al. 1997). Type III collagen is a fibrillar forming collagen comprising three alpha-1 (III) chains and is expressed in early embryos and throughout embryogenesis. In the adult, type III collagen is a component of the ECM in a variety of internal organs and skin. Patients with type IV Ehlers–Danlos syndrome, a genetic disorder associated with fragile blood vessels and skin, often carry mutations in the COL3A1 gene encoding for type III procollagen (Kontusaari et al. 1990; Kuivaniemi et al. 1995; Prockop and Kivirikko 1984). Type III collagen is important for the development of skin and the cardiovascular system and for maintaining the normal physiological functions of these organs in adult life (Olsen 1995). In addition, type III collagen is known to be prominent at sites of healing and repair in skin and other tissues (Wu et al. 2010). Type III collagen is the major constituent of early granulation and scar tissue, whereas only a small amount of type I collagen is present in this early phase of healing (Betz et al. 1993; El Sherif et al. 2006). On the other hand, type I collagen is a major fibrous component in connective tissue. During the wound healing process, type I collagen accumulates in granulation tissue (Kanzler et al. 1986). Because the expression of type III collagen is usually greater than the expression of type I collagen during early wound healing, the lower ASESM-PMBN in vitro system might provide an ECM environment similar to that of the early phase of wound healing.

Decorin belongs to the small leucine-rich proteoglycans (SLRPs), which are expected to play important functions in tissue assembly. Danielson et al.(1997) have reported that mice possessing a targeted disruption of the decorin gene

are viable but have fragile skin with markedly reduced tensile strength. Since the repair of wound healing is delayed in the decorin-knockout mouse, decorin proteogrican is necessary for the wound healing process (Jarvelainen et al. 2006). In keloid scars seen in deregulated wound healing, decorin expression is downregulated, whereas syndecan-2 and fibroblast growth factor-2 (FGF-2) are upregulated (Mukhopadhyay et al. 2010). In addition, the activation of extracellular signal-regulated kinase-1 (ERK1) and ERK2 and the lower expression of decorin are found in the fibroblasts of the dermal region in keloids (Meenakshi et al. 2009). On the other hand, the overexpression of the decorin gene in human corneal fibroblasts inhibits transforming growth factor-β (TGF-β)-induced fibrosis and myofibroblast formation (Mohan et al. 2010). These reports suggest that decorin has an antifibrotic effect in an aberrant wound healing process leading to keloid scars.

MMPs play a role in various aspects of cutaneous biology and pathology, e.g., in wound repair. MMP2 is expressed in the early phase (7th day) of wound healing (Jansen et al. 2007). MMP2 expression is high in low-dose ASESM in our in vitro system. MMP2 degrades various ECM molecules, such as collagen types I, IV, V, VII, and X, gelatin, fibronectin, tenascin, fibrillin, osteonectin, entactin, aggrecan, vitronectin, and decorin (Kerkela and Saarialho-Kere 2003) and is activated by dermatan sulfate (Isnard et al. 2003). Since dermatan sulfate is reported to be one of the components of ESM (Osuoji 1971), it is also present in our ASESM system and might contributed to MMP2 activation. MMP2 seems to be a key molecule for tissue remodeling, as demonstrated by Tholozan et al. (2007) who have shown that lens epithelial cells produce several MMPs including MMP2, which releases FGF-2 from the lens capsule. In this system, the recently proposed ECM reservoir hypothesis has been established, because the ECM itself can act as a reservoir for growth and survival factors that are released via the action of various MMPs such as MMP2 (Tholozan et al. 2007). Thus, lower density cell culture on low ASESM might provide a good environment for wound healing without leading to keloid scar formation during tissue regeneration.

In vivo, fibroblast cells are located separated from each other, which differs from the situation for keratinocytes in the epidermis. As described above, collagen type III, decorin, and MMP2 play an important role in wound healing, type I collagen fibrogenesis, and the maintenance and turnover of the ECM environment during skin damage. In this study, sparsely located HDF show an unextended-shape on a low-dose ASESM matrix, whereas the mRNA expression levels of type III collagen, MMP2, and decorin markedly increase more than two-fold compared with those of cells grown on control TC or collagen-coated dishes. The proteins encoded by these ECM genes are key molecules for remodeling of ECM in wounded and developing dermis and contribute to keeping the skin healthy. However, the precise mechanisms of their involvement are largely unknown.

HDF express collagen type III, MMP2, and decorin mRNA at a higher level on a low dose of ASESM, but the levels of collagen type I, elastin, MMP3, and biglycan are not significantly altered. Biglycan belongs to the group of small leucine-rich proteoglycans, as does decorin, and decorates collagen during fibrogenesis (Corsi et al. 2002). Decorin and biglycan expression patterns are reported to be differentially regulated during wound healing. In dermal fibroblast cultures, decorin expression is stimulated by glycyl-histidyl-lysine-Cu^{2+}, which is a tripeptide isolated from human plasma and a potent activator of wound healing. In contrast, biglycan expression is not modified (Pickart and Thaler 1973). In addition, the inactivation of the decorin gene by homologous recombination (Danielson et al. 1997; Xu et al. 1998), but not that of biglycan (Simeon et al. 2000), is associated with a fragile skin collagen network. A previous study has also revealed few changes occur with regard to biglycan expression through 1–49 days of the wound healing process in pig (Wang et al. 2000). Thus, we can reasonably conclude that different regulatory mechanism are also involved in the patterns of expression of decorin and biglycan in our system, despite both belonging to the small leucine-rich proteoglycans.

Elastin, which constitutes elastic fibers in the dermis, blood vessel, and lung (Rosenbloom et al. 1993), did not change its expression level related to ASESM quantity in this study. However, a relatively low expression level was observed under lower dose ASESM conditions. A previous study has indicated that elastin expression increases during the early phase of wound healing (Quaglino et al. 1990). Basic fibroblastic growth factor has been reported to be of importance in the regulation of ECM gene expression, such as the decrease of elastin expression (Debelle and Tamburro 1999) but increase of type III collagen and decorin (Li et al. 2009; Tan et al. 1993). Although growth factors/cytokines were not measured in this study, the dose-dependent change of ECM mRNA may well reflect the ECM-cytokine relationship during wound healing described in previous reports.

The expression pattern of MMP3 mRNA at the different ASESM concentrations are a mirror image of the pattern of elastin expression. MMP3 is secreted mainly by macrophages and fibroblast cells (Saarialho-Kere et al. 1994; Welgus et al. 1990; Wilhelm et al. 1987) and digest a broad range of ECM molecules, such as type I collagen, various proteoglycans, and others (ColIII, IV, V, VII, IX, and X, elastin, fibronectin, fibrillin, fibrinogen, gelatin, aggrecan, plasmin, kallikrein, chymase,LN-1, nidogen, vitronectin, osteonectin, decorin; Kerkela and Saarialho-Kere 2003), as substrates. The higher MMP3 mRNA expression either at

low ASESM (ASESM at 1, 5, 10 mg/ml) or high ASESM (ASESM at 100 mg/ml) might indicate that ECM turnover is high under these conditions. Delayed and incomplete wound healing is observed in the MMP3-knockout mouse resulting from insufficient myofibroblast migration or differentiation. Therefore, MMP3 function is important for proper wound healing, and our ASESM system provides the necessary environment.

Interestingly, a large difference has been noted in HDF cell shape between low- and high-dose ASESM (Figs. 2, 5b, c), suggesting that different actin dynamics and related signal transduction mechanisms are involved in the two states. Hyaluronan expression level seems to change in relation to the cellular and extracellular metabolism and to the immune system through actin dynamics (Boraldi et al. 2003; Stern 2003). Particle-exclusion assay in this study shows water-binding ECM surrounding HDF cells grwon on both low and high dose ASESM. The distance of the water-binding ECM from the cell surface to the excluded erythrocyte is similar between low and high ASESM. This data suggest that HDF on the ASESM surface secretes enough pericellular coat, including GAG-bound proteoglycan and hyaluronan, at a low dose of ASESM and at a high dose of ASESM. The pericellular hyaluronan coat requires TGF-β expression (Simpson et al. 2009). The differentiation of fibroblasts to myofibroblasts during wound healing needs the expression of epidermal growth factor receptor and ERK1/2, and smooth-muscle α-actin, which is a marker of myofibroblasts (Simpson et al. 2009). Type III collagen has an important role in wound healing, because the expression of type III collagen increases early during wound healing processes (Liu et al. 1995). Human fibroblasts with mutations in the COL5A1 and COL3A1 genes do not organize collagens and fibronectin in the ECM, down-regulate α2β1 integrin, and recruit αvβ3 instead of α5β1 integrin (Zoppi et al. 2004). The αvβ3 receptor (vitronectin receptor) and the α5β1 receptor (fibronectin receptor) have been shown to be important in myofibroblast differentiation (Lygoe et al. 2007). Mice deficient in type III collagen have an increased myofibroblast density in the wound granulation tissue, as evidenced by the increased expression of the myofibroblast marker, smooth-muscle α-actin, and wounds in such mice have significantly more scar tissue area compared with that of wild-type mice (Volk et al. 2011). In our study, HDF cultured on the low-dose ASESM environment induce a cytoskeletal rearrangement and change the expression of ECM, especially type III collagen, by affecting the interaction with integrin. We hypothesize that the newly designed PMBN-ASESM biointerface mimicks the microenvironment of both early and late remodeling in the wound healing process.

The inductive mechanism of these highly expressed genes (type III collagen, decorin, and MMP2) in HDF on the low dose of ASESM seems to be related to the cell shape, cellular environment, cell-cell interaction (low or high cell density), and ECM components or its structure. Because the high dose of ASESM does not activate these three genes, regardless of the cell density, we suggest that the particular ECM environment that is mediated by the low ASESM dose plays a pivotal role for the observed cell adhesion mode and therefore affects the gene expression pattern. ASESM, the hydrolyzed material of ESM, might contain the ECM-related molecules and MMPs as regulatory factors. We hypothesize that HDF secrete exactly the same or similar ECM proteins to those of the surrounding ECM, because fibroblasts are known to be responsive to various signals (Discher et al. 2005). Cells express the corresponding genes in response to their surrounding environment and to environmental stimuli (mechanical force or UV stress, etc.). Cells and ECM interact with each other and adapt to their environment. If the environment of the cells is adequate, they can maintain the optimal condition for their survival. Mesenchymal stem cells retain their pluripotency providing that the surrounding environment remains suitable for stem cells.

In this study, the three genes (type III collagen, decorin, and MMP2) that are expressed in younger skin or early wound healing process are highly expressed by HDF on low doses of ASESM. This probably occurs because the required structure pre-exists or is assembled de novo on PMBN.

ESM might contain almost all ECMs and ECM-regulatory gene products that have been evolutionally conserved in avians. Previous studies have shown that ESMs have a fibrous network mainly comprised of type I, V, and X collagen, glucosamine, desmosin, hyaluronic acid (Ha et al. 2007; Osuoji 1971; Wong et al. 1984); because these molecules are cross-linked by lysyl oxidase (Harris et al. 1980), each component in ESMs cannot exist independently. In the low concentration solution (low-dose ASESM), hydrophilic small molecules that are produced by the moderately alkaline hydrolyzed ESM might be assembled in such a manner that a large amount of water surrounds it, thereby creating an ECM environment that mimicks younger skin. In contrast, the high concentration of ASESM (high-dose ASESM) might induce the self-assembly of the ASESM components, such as the more hydrophobic ECM molecules (collagens) that relatively easily exclude water.

Such a self-assembly of macromolecules (ECM-related fibrils) might be involved during embryonic development and wound healing process in the animal body. By using a novel combination of a natural (ESM) and artificial cell membrane interface (PMBN), ECM components in ESM might be able to self-assemble differently and provide a distinct ECM environment depending on the ASESM concentration. Thus, the cells adhere to the respective environment and express the observed ECM components. The ASESM-PMBN system in this study should be

applicable in various mechanistic studies of biological processes, such as wound healing, embryonic development, acquisition of tissue specificity, evolution and morphogenesis, at the molecular level.

In conclusion, ASESM has been stably conjugated to PMBN and provides an ECM environment for HDF. ESM also acts as a scaffold for eggshell mineralization and might have properties for capturing various factors and molecules that are necessary for avian embryonic development. Recently, a clinical evaluation of natural ESM has also reported joint and muscle pain relief (Ruff et al. 2009a, b). Although the immobilization of knee joints induces articular contracture associated with sequential changes of disordered ECM alignment, increased collagen glycation with pentosidine, and decreased cell numbers (Lee et al. 2010), the possible in vivo application of ASESM might not only stabilize connective tissues such as joints, but also stimulate ECM production therein. Further study of the ASESM-PMBN system with respect not only to skin wound healing, but also to the treatment of joint pain such as osteoarthritis should be considered, as MPC polymer has been shown to improve the surface grafting of artificial joints dramatically (Moro et al. 2004) and is under clinical trial awaiting biomedical use. In addition, our ASESM-PMBN system provides a rare experimental model for studying a mutually dynamic biological process in vitro: the cell responds to the surrounding microenvironment by secreting an ECM, and vice versa, the environment stimulates the cell.

Acknowledgements We appreciate the valuable comments of the reviewers. We thank the Radio Isotope Center and Center for NanoBio Integration (CNBI), The University of Tokyo for the use of analytical equipment, and we are grateful to Prof. Yoshihiko Nakamura at The University of Tokyo for administration of the "Cell to Body Dynamics Project", which included this ESM cooperative project.

References

Ahlborn G, Sheldon BW (2005) Enzymatic and microbiological inhibitory activity in eggshell membranes as influenced by layer strains and age and storage variables. Poult Sci 84:1935–1941

Aiba-Kojima E, Tsuno NH, Inoue K, Matsumoto D, Shigeura T, Sato T, Suga H, Kato H, Nagase T, Gonda K, Koshima I, Takahashi K, Yoshimura K (2007) Characterization of wound drainage fluids as a source of soluble factors associated with wound healing: comparison with platelet-rich plasma and potential use in cell culture. Wound Repair Regen 15:511–520

Betz P, Nerlich A, Wilske J, Tubel J, Penning R, Eisenmenger W (1993) Analysis of the immunohistochemical localization of collagen type III and V for the time-estimation of human skin wounds. Int J Leg Med 105:329–332

Boraldi F, Croce MA, Quaglino D, Sammarco R, Carnevali E, Tiozzo R, Pasquali-Ronchetti I (2003) Cell-matrix interactions of in vitro human skin fibroblasts upon addition of hyaluronan. Tissue Cell 35:37–45

Bruckner P (2010) Suprastructures of extracellular matrices: paradigms of functions controlled by aggregates rather than molecules. Cell Tissue Res 339:7–18

Burley RW, Vadehra DV (1989) The avian egg, chemistry and biology. Wiley, New York

Corsi A, Xu T, Chen XD, Boyde A, Liang J, Mankani M, Sommer B, Iozzo RV, Eichstetter I, Robey PG, Bianco P, Young MF (2002) Phenotypic effects of biglycan deficiency are linked to collagen fibril abnormalities, are synergized by decorin deficiency, and mimic Ehlers-Danlos-like changes in bone and other connective tissues. J Bone Miner Res 17:1180–1189

Danielson KG, Baribault H, Holmes DF, Graham H, Kadler KE, Iozzo RV (1997) Targeted disruption of decorin leads to abnormal collagen fibril morphology and skin fragility. J Cell Biol 136:729–743

Debelle L, Tamburro AM (1999) Elastin: molecular description and function. Int J Biochem Cell Biol 31:261–272

Diegelmann RF, Evans MC (2004) Wound healing: an overview of acute, fibrotic and delayed healing. Front Biosci 9:283–289

Discher DE, Janmey P, Wang YL (2005) Tissue cells feel and respond to the stiffness of their substrate. Science 310:1139–1143

El Sherif A, Yano F, Mittal S, Filipi CJ (2006) Collagen metabolism and recurrent hiatal hernia: cause and effect? Hernia 10:511–520

Evanko SP, Angello JC, Wight TN (1999) Formation of hyaluronan- and versican-rich pericellular matrix is required for proliferation and migration of vascular smooth muscle cells. Arterioscler Thromb Vasc Biol 19:1004–1013

Grzesiak JJ, Pierschbacher MD, Amodeo MF, Malaney TI, Glass JR (1997) Enhancement of cell interactions with collagen/glycosaminoglycan matrices by RGD derivatization. Biomaterials 18:1625–1632

Ha YW, Son MJ, Yun KS, Kim YS (2007) Relationship between eggshell strength and keratan sulfate of eggshell membranes. Comp Biochem Physiol A Mol Integr Physiol 147:1109–1115

Harris ED, Blount JE, Leach RM Jr (1980) Localization of lysyl oxidase in hen oviduct: implications in egg shell membrane formation and composition. Science 208:55–56

Ino T, Hattori M, Yoshida T, Hattori S, Yoshimura K, Takahashi K (2006) Improved physical and biochemical features of a collagen membrane by conjugating with soluble egg shell membrane protein. Biosci Biotechnol Biochem 70:865–873

Isnard N, Robert L, Renard G (2003) Effect of sulfated GAGs on the expression and activation of MMP-2 and MMP-9 in corneal and dermal explant cultures. Cell Biol Int 27:779–784

Itano N, Sawai T, Yoshida M, Lenas P, Yamada Y, Imagawa M, Shinomura T, Hamaguchi M, Yoshida Y, Ohnuki Y, Miyauchi S, Spicer AP, McDonald JA, Kimata K (1999) Three isoforms of mammalian hyaluronan synthases have distinct enzymatic properties. J Biol Chem 274:25085–25092

Jansen PL, Rosch R, Jansen M, Binnebosel M, Junge K, Alfonso-Jaume A, Klinge U, Lovett DH, Mertens PR (2007) Regulation of MMP-2 gene transcription in dermal wounds. J Invest Dermatol 127:1762–1767

Jarvelainen H, Puolakkainen P, Pakkanen S, Brown EL, Hook M, Iozzo RV, Sage EH, Wight TN (2006) A role for decorin in cutaneous wound healing and angiogenesis. Wound Repair Regen 14:443–452

Kahari VM, Saarialho-Kere U (1997) Matrix metalloproteinases in skin. Exp Dermatol 6:199–213

Kanzler MH, Gorsulowsky DC, Swanson NA (1986) Basic mechanisms in the healing cutaneous wound. J Dermatol Surg Oncol 12:1156–1164

Kerkela E, Saarialho-Kere U (2003) Matrix metalloproteinases in tumor progression: focus on basal and squamous cell skin cancer. Exp Dermatol 12:109–125

Kim SG, Akaike T, Sasagaw T, Atomi Y, Kurosawa H (2002) Gene expression of type I and type III collagen by mechanical stretch in anterior cruciate ligament cells. Cell Struct Funct 27:139–144

Konno T, Watanabe J, Ishihara K (2004) Conjugation of enzymes on polymer nanoparticles covered with phosphorylcholine groups. Biomacromolecules 5:342–347

Kontusaari S, Tromp G, Kuivaniemi H, Romanic AM, Prockop DJ (1990) A mutation in the gene for type III procollagen (COL3A1) in a family with aortic aneurysms. J Clin Invest 86:1465–1473

Kuivaniemi H, Tromp G, Bergfeld WF, Kay M, Helm TN (1995) Ehlers-Danlos syndrome type IV: a single base substitution of the last nucleotide of exon 34 in COL3A1 leads to exon skipping. J Invest Dermatol 105:352–356

Laurent TC, Fraser JR (1992) Hyaluronan. FASEB J 6:2397–2404

Lee S, Sakurai T, Ohsako M, Saura R, Hatta H, Atomi Y (2010) Tissue stiffness induced by prolonged immobilization of the rat knee joint and relevance of AGEs (pentosidine). Connect Tissue Res 51:467–477

Li F, Fan C, Cheng T, Jiang C, Zeng B (2009) Efficient inhibition of fibroblast proliferation and collagen expression by ERK2 siRNAs. Biochem Biophys Res Commun 382:259–263

Liu SH, Yang RS, al-Shaikh R, Lane JM (1995) Collagen in tendon, ligament, and bone healing. A current review. Clin Orthop Relat Res 318:265–278

Liu X, Wu H, Byrne M, Krane S, Jaenisch R (1997) Type III collagen is crucial for collagen I fibrillogenesis and for normal cardiovascular development. Proc Natl Acad Sci USA 94:1852–1856

Lygoe KA, Wall I, Stephens P, Lewis MP (2007) Role of vitronectin and fibronectin receptors in oral mucosal and dermal myofibroblast differentiation. Biol Cell 99:601–614

Meenakshi J, Vidyameenakshi S, Ananthram D, Ramakrishnan KM, Jayaraman V, Babu M (2009) Low decorin expression along with inherent activation of ERK1,2 in ear lobe keloids. Burns 35:519–526

Mohan RR, Gupta R, Mehan MK, Cowden JW, Sinha S (2010) Decorin transfection suppresses profibrogenic genes and myofibroblast formation in human corneal fibroblasts. Exp Eye Res 91:238–245

Moro T, Takatori Y, Ishihara K, Konno T, Takigawa Y, Matsushita T, Chung UI, Nakamura K, Kawaguchi H (2004) Surface grafting of artificial joints with a biocompatible polymer for preventing periprosthetic osteolysis. Nat Mater 3:829–836

Mukhopadhyay A, Wong MY, Chan SY, Do DV, Khoo A, Ong CT, Cheong HH, Lim IJ, Phan TT (2010) Syndecan-2 and decorin: proteoglycans with a difference—implications in keloid pathogenesis. J Trauma 68:999–1008

Nomura Y (2006) Structural change in decorin with skin aging. Connect Tissue Res 47:249–255

Olsen BR (1995) The roles of collagen genes in skeletal development and morphogenesis. Experientia 51:194–195

Osuoji CI (1971) Acid glycosaminoglycan of eggshell membranes. Biochim Biophys Acta 244:481–483

Pickart L, Thaler MM (1973) Tripeptide in human serum which prolongs survival of normal liver cells and stimulates growth in neoplastic liver. Nat New Biol 243:85–87

Prockop DJ, Kivirikko KI (1984) Heritable diseases of collagen. N Engl J Med 311:376–386

Quaglino D Jr, Nanney LB, Kennedy R, Davidson JM (1990) Transforming growth factor-beta stimulates wound healing and modulates extracellular matrix gene expression in pig skin. I. Excisional wound model. Lab Invest 63:307–319

Rinn JL, Wang JK, Liu H, Montgomery K, Rijn M van de, Chang HY (2008) A systems biology approach to anatomic diversity of skin. J Invest Dermatol 128:776–782

Rose ML, Hincke MT (2009) Protein constituents of the eggshell: eggshell-specific matrix proteins. Cell Mol Life Sci 66:2707–2719

Rosenbloom J, Abrams WR, Mecham R (1993) Extracellular matrix 4: the elastic fiber. FASEB J 7:1208–1218

Ruff KJ, DeVore DP, Leu MD, Robinson MA (2009a) Eggshell membrane: a possible new natural therapeutic for joint and connective tissue disorders. Results from two open-label human clinical studies. Clin Interv Aging 4:235–240

Ruff KJ, Winkler A, Jackson RW, DeVore DP, Ritz BW (2009b) Eggshell membrane in the treatment of pain and stiffness from osteoarthritis of the knee: a randomized, multicenter, double-blind, placebo-controlled clinical study. Clin Rheumatol 28:907–914

Saarialho-Kere UK, Pentland AP, Birkedal-Hansen H, Parks WC, Welgus HG (1994) Distinct populations of basal keratinocytes express stromelysin-1 and stromelysin-2 in chronic wounds. J Clin Invest 94:79–88

Simeon A, Wegrowski Y, Bontemps Y, Maquart FX (2000) Expression of glycosaminoglycans and small proteoglycans in wounds: modulation by the tripeptide-copper complex glycyl-L-histidyl-L-lysine-Cu(2+). J Invest Dermatol 115:962–968

Simpson RM, Meran S, Thomas D, Stephens P, Bowen T, Steadman R, Phillips A (2009) Age-related changes in pericellular hyaluronan organization leads to impaired dermal fibroblast to myofibroblast differentiation. Am J Pathol 175:1915–1928

Stern R (2003) Devising a pathway for hyaluronan catabolism: are we there yet? Glycobiology 13:105R–115R

Takahashi K, Yamanaka S (2006) Induction of pluripotent stem cells from mouse embryonic and adult fibroblast cultures by defined factors. Cell 126:663–676

Tan EM, Hoffren J, Rouda S, Greenbaum S, Fox JWt, Moore JH Jr, Dodge GR (1993) Decorin, versican, and biglycan gene expression by keloid and normal dermal fibroblasts: differential regulation by basic fibroblast growth factor. Exp Cell Res 209:200–207

Tholozan FM, Gribbon C, Li Z, Goldberg MW, Prescott AR, McKie N, Quinlan RA (2007) FGF-2 release from the lens capsule by MMP-2 maintains lens epithelial cell viability. Mol Biol Cell 18:4222–4231

Tsang KY, Cheung MC, Chan D, Cheah KS (2010) The developmental roles of the extracellular matrix: beyond structure to regulation. Cell Tissue Res 339:93–110

Vitellaro-Zuccarello L, Garbelli R, Rossi VD (1992) Immunocytochemical localization of collagen types I, III, IV, and fibronectin in the human dermis. Modifications with ageing. Cell Tissue Res 268:505–511

Volk SW, Wang Y, Mauldin EA, Liechty KW, Adams SL (2011) Diminished type III collagen promotes myofibroblast differentiation and increases scar deposition in cutaneous wound healing. Cells Tissues Organs (in press)

von der Mark K, Park J, Bauer S, Schmuki P (2010) Nanoscale engineering of biomimetic surfaces: cues from the extracellular matrix. Cell Tissue Res 339:131–153

Wang JF, Olson ME, Reno CR, Kulyk W, Wright JB, Hart DA (2000) Molecular and cell biology of skin wound healing in a pig model. Connect Tissue Res 41:195–211

Watanabe J, Ishihara K (2007) Multiple protein-immobilized phospholipid polymer nanoparticles: effect of spacer length on residual enzymatic activity and molecular diagnosis. Nanobiotechnol 3:76–82

Welgus HG, Campbell EJ, Cury JD, Eisen AZ, Senior RM, Wilhelm SM, Goldberg GI (1990) Neutral metalloproteinases produced by human mononuclear phagocytes. Enzyme profile, regulation, and expression during cellular development. J Clin Invest 86:1496–1502

Wilhelm SM, Collier IE, Kronberger A, Eisen AZ, Marmer BL, Grant GA, Bauer EA, Goldberg GI (1987) Human skin fibroblast stromelysin: structure, glycosylation, substrate specificity, and differential expression in normal and tumorigenic cells. Proc Natl Acad Sci USA 84:6725–6729

Wong M, Hendrix MJ, Mark K von der, Little C, Stern R (1984) Collagen in the egg shell membranes of the hen. Dev Biol 104:28–36

Wu JJ, Weis MA, Kim LS, Eyre DR (2010) Type III collagen, a fibril network modifier in articular cartilage. J Biol Chem 285:18537–18544

Xu T, Bianco P, Fisher LW, Longenecker G, Smith E, Goldstein S, Bonadio J, Boskey A, Heegaard AM, Sommer B, Satomura K, Dominguez P, Zhao C, Kulkarni AB, Robey PG, Young MF (1998) Targeted disruption of the biglycan gene leads to an osteoporosis-like phenotype in mice. Nat Genet 20:78–82

Zhang L, Tran N, Chen HQ, Kahn CJ, Marchal S, Groubatch F, Wang X (2008) Time-related changes in expression of collagen types I and III and of tenascin-C in rat bone mesenchymal stem cells under co-culture with ligament fibroblasts or uniaxial stretching. Cell Tissue Res 332:101–109

Zoppi N, Gardella R, De Paepe A, Barlati S, Colombi M (2004) Human fibroblasts with mutations in COL5A1 and COL3A1 genes do not organize collagens and fibronectin in the extracellular matrix, down-regulate alpha2beta1 integrin, and recruit alphavbeta3 instead of alpha5beta1 integrin. J Biol Chem 279:18157–18168